y-scaling analysis of quasielastic electron scattering and nucleon momentum distributions in few-body systems, complex nuclei, and nuclear matter

C. Ciofi degli Atti,[1,2] E. Pace,[1,3] and G. Salmè[1]

[1]*Istituto Nazionale di Fisica Nucleare, Sezione Sanità, V. le Regina Elena 299,
I-00161 Roma, Italy*

[2]*Department of Physics, University of Perugia, V. A. Pascoli, I-06100 Perugia, Italy*

[3]*Dipartimento di Fisica, Università di Roma "Tor Vergata", Via E. Carnevale,
I-00173 Roma, Italy*

(Received 7 August 1990)

The approach to y scaling previously adopted to obtain the nucleon momentum distribution in the two- and three-nucleon systems is extended to the case of complex nuclei and nuclear matter. The basic elements of this approach, which takes properly into account nucleon binding and momentum, are reviewed. A new method of analysis, which allows one to obtain the experimental asymptotic scaling function from inclusive cross sections even if these data are affected by final-state interactions, is proposed and illustrated. By such a method, the asymptotic scaling functions of ^{3}He, ^{4}He, ^{12}C, ^{56}Fe, and nuclear matter are obtained from recent experimental data and it is demonstrated that, particularly at high negative values of the scaling variable, the available data points at the highest value of the momentum transfer are affected by final-state interaction and cannot therefore be considered to represent the asymptotic scaling function. It is shown that, unlike what is commonly stated, the nucleon momentum distribution is not simply defined in terms of the derivative of the asymptotic scaling function, but as a sum of such a derivative plus the derivative of a quantity, the binding correction, generated by the removal energy distribution of nucleons embedded in the nuclear medium. The binding correction and its derivative are evaluated with various types of spectral functions, and the nucleon momentum distributions in ^{3}He, ^{4}He, ^{12}C, ^{56}Fe, and nuclear matter are obtained up to nucleon momenta $k \approx 500$ MeV/c. For few-body systems the obtained momentum distributions satisfactorily agree with the ones extracted from $(e,e'p)$ reactions and with theoretical calculations performed within Faddeev or variational approaches, whereas for complex nuclei they qualitatively agree with predictions of theoretical many-body approaches which take nucleon-nucleon correlations into account and, at the same time, at $k \geq 350$ MeV/c they are larger by orders of magnitude than the ones predicted by mean field approaches. Such a result does represent unambiguous evidence of correlation effects in nuclei.

I. INTRODUCTION

Since the pioneering work by West,[1] there was a growth of interest in y scaling, both in its experimental and theoretical aspects. The central issue in this field concerns the question as to whether the analysis of quasielastic inclusive electron scattering data in terms of y scaling can provide nontrivial information on the properties of nucleons embedded in the nuclear medium. In this regard, one of the main expectations concerns the possibility of obtaining information on the nucleon momentum distribution $n(k)$. This quantity plays a crucial role in understanding the structure of many-body systems and in particular of atomic nuclei, for it provides unique information on nucleon-nucleon (NN) correlations (see, e.g., Refs. 2–6). As a matter of fact, under certain stringent assumptions, namely, the validity of the plane-wave impulse approximation (PWIA) and the use of nonrelativistic kinematics to describe the scattering process, it can be shown that the asymptotic scaling function coincides with the longitudinal momentum distribution.[1,7] Such a simple picture, however, is no longer valid if relativistic kinematics is adopted to describe the scattering process;[8] moreover, the corrections to the PWIA, like, e.g., the final-state interaction (FSI), may strongly affect quasielastic scattering at finite values of the momentum transfer,[9–14] and its effects have also been advocated even in the asymptotic limit,[13,15] although only in the case of particles interacting via hard core potentials. From an experimental point of view, the possibility of extracting the nucleon momentum distribution from qe inclusive data, relies on the knowledge of the scaling function in the asymptotic limit, and no clear cut criteria exist to date to decide whether the available data, which are necessarily obtained at large, but finite values of the momentum transfer, can be associated with the true asymptotic region. It would appear, therefore, that the extraction of the momentum distribution from y scaling is not an easy task. Nonetheless, in view of the basic necessity of the experimental knowledge of the nucleon momentum distribution, serious efforts are worth being done in order to clearly understand if, and to what extent, such a quantity can be obtained from quasielastic data.

In two previous papers of ours,[16,17] it has been shown

that if a proper theory of y scaling, which takes into account nucleon binding and momentum, is adopted, quasielastic experimental electron scattering cross sections at high momentum transfer from ^2H (Ref. 18) and ^3He (Ref. 19) allow one to extract nucleon momentum distributions which satisfactorily agree with those obtained in a more direct way from exclusive $(e,e'p)$ experiments,[20,21] thus confirming the expectation that the nucleon momentum distribution can indeed be obtained from a y-scaling analysis of inclusive cross sections. In view of the recent appearance of experimental data for ^4He, ^{12}C, ^{56}Fe (Ref. 22), and of extrapolated data for nuclear matter[23] in the low-energy side of the quasielastic peak, where y scaling is expected to be observed, we have extended to complex nuclei the approach of Refs. 16 and 17. The approach has moreover been implemented in such a way as to obtain a model-independent determination of the asymptotic value of the scaling function from the experimental data obtained at high, but finite values of the momentum transfer, even if these data are affected by the final-state interaction. Our approach allows one to obtain the asymptotic value of the scaling function without the need of data at very high momentum transfer, where the dominant contributions from inelastic and deep inelastic scattering by the nucleon will hinder the extraction of the quasielastic contribution.

The main outcome of our work is that the nucleon momentum distribution in complex nuclei can be determined up to $k \approx 500$ MeV/c, using the present (e,e') experimental data. This result appears to be a relevant one, for in the region 300 MeV/$c \leq k \leq 500$ MeV/c exclusive $(e,e'p)$ experiments on complex nuclei have not yet been performed and, more important, theoretical predictions by mean field approaches differ by orders of magnitude from the predictions of approaches where the effects of NN correlations are taken into account. Our results allow one to conclude that for $k \geq 300$ MeV/c the nucleon momentum distribution is almost entirely determined by the effects of NN correlations, in agreement with recent theoretical predictions.[2-6]

Our paper is organized as follows. In Section II the definition and the physical meaning of the scaling variable and the scaling function will be briefly reviewed; in Sec. III the nucleon spectral function and its relations with the scaling function and the momentum distribution will be illustrated; in Sec. IV the new approach for obtaining the asymptotic scaling function and the nucleon momentum distribution will be described; in Sec. V the nucleon momentum distributions in ^3He, ^4He, ^{12}C, ^{56}Fe, and nuclear matter will be presented; in Sec. VI the general features of the nucleon momentum distributions resulting from many-body calculations and from our y-scaling analysis will be discussed; the summary and the conclusions are presented in Sec. VII.

II. THE SCALING FUNCTION AND THE SCALING VARIABLE: THEIR DEFINITION AND PHYSICAL MEANING

The general concepts of y scaling in quasielastic electron scattering by nuclei have been introduced by West,[1] who has developed an approach aimed at establishing a relation between the scaling function and the form of the NN interaction (for recent developments along this line, see Refs. 24 and 13). The basic assumptions underlying West's approach are (1) one-photon-exchange approximation; (2) only the nucleon degrees of freedom are considered; (3) after interaction with the photon, a nucleon with momentum $\mathbf{k}$ undergoes a transition from the free state with kinetic energy $T_1 = k^2/2M$ to the free state with kinetic energy $T_2 = (\mathbf{k}+\mathbf{q})^2/2M$, q being the three-momentum transfer; (4) the convective current in the electron-nucleon cross section is disregarded; (5) nonrelativistic kinematics is used. Within these approximations, it has been shown[1] that the inclusive cross section factorizes into the elementary electron-nucleon cross section, a kinematical factor and a function f (the scaling function) of the variable y_0 (West's scaling variable), which represents the longitudinal (along q) momentum component of a nucleon embedded in a Fermi gas, viz. $y_0 = (\mathbf{q} \cdot \mathbf{k})/q = (M/q)(\omega - q^2/2M)$; the scaling function itself is

$$f(y_0) = 2\pi \int_{|y_0|}^{\infty} n_{FG}(k) k \, dk \, , \tag{1}$$

i.e., the longitudinal momentum distribution of a nucleon with Fermi gas momentum distribution $n_{FG}(k)$.

An approach to y scaling, aimed at considering the momentum and energy distributions of nucleons in a system of interacting particles, as well as relativistic kinematics to describe the scattering process, has been proposed by the present authors within the PWIA. This paper is based on such an approach, whose main assumptions and features will be recalled here below (for more details, see, e.g., Ref. 25). In our theory of y scaling, the momenta of the bound nucleons and their separation energies are correctly taken into account, unlike approximate versions of y scaling, where the separation energy and the perpendicular momentum component have been disregarded,[26] with a resulting ambiguous definition of the scaling function and the scaling variable. In this regard, it should be pointed out that at present there is a general consensus[27-31] as far as the definition of the scaling function as given in Ref. 25 is concerned.

A. The plane-wave impulse approximation cross section

The inclusive electron scattering cross section describing, in PWIA, the knock out of a nucleon N from a nucleus A, is

$$\sigma_2(q,\omega) \equiv \frac{d^2\sigma(q,\omega)}{d\omega \, d\Omega} = \sum_{N=1}^{A} \int dE \int d^3k \, P_N(k,E) \sigma_{eN} \delta[\omega + M_A - E_2(k_N) - E_R(k_R)] \, , \tag{2}$$

where ω is the energy transfer, $q \equiv |\mathbf{q}|$ the three-momentum transfer, $\mathbf{k} = \mathbf{k}_N - \mathbf{q}$ the nucleon momentum before interaction, $E = E_{\min} + E_{A-1}^{f*}$ the nucleon removal energy [$E_{\min} = M + M_{A-1} - M_A$ and E_{A-1}^{f*} is the excitation energy of the final $(A-1)$ nucleon system], $E_2(k_N) = [M^2 + (\mathbf{k}+\mathbf{q})^2]^{1/2}$ the nucleon energy in the final state, $\mathbf{k}_R = -\mathbf{k}$ and

$E_R(k_R) = [(M_{A-1} + E^{f*}_{A-1})^2 + k^2]^{1/2}$ the momentum and energy of the recoiling final $(A-1)$ system, and, finally, $\sigma_{eN} = \sigma_{eN}(q, \omega, \mathbf{k}, E)$ the relativistic electron-nucleon cross section for the scattering of an electron by an off-shell nucleon with momentum $\mathbf{k}$. In Eq. (2), $P_N(k, E)$ is the nucleon *spectral function*, which represents the joint probability distribution to find in the target nucleus a nucleon with momentum k and removal energy E or, equivalently, the joint probability distribution that, after a nucleon with momentum k has been removed from the target, the $(A-1)$-nucleon system is left with excitation energy E^{f*}_{A-1}. By disregarding, for ease of presentation, any difference between the proton and the neutron spectral functions, $P(k, E)$ can be defined as follows

$$P(k,E) = \frac{1}{2J+1} \sum_{M,\sigma} \langle \Psi^{JM}_A | a^+_{\mathbf{k}\sigma} \delta[E - (H - E_A)] a_{\mathbf{k}\sigma} | \Psi^{JM}_A \rangle$$

$$= \frac{1}{2J+1} \sum_{M,\sigma} \Sigma_f | \langle \Psi^f_{A-1} | a_{\mathbf{k}\sigma} | \Psi^{JM}_A \rangle |^2 \delta[E - (E^f_{A-1} - E_A)]$$

$$= \frac{1}{2J+1} (2\pi)^{-3} \sum_{M,\sigma} \Sigma_f \left| \int d\mathbf{z}\, e^{i\mathbf{k}\cdot\mathbf{z}} G^{M\sigma}_f(\mathbf{z}) \right|^2 \delta[E - (E^f_{A-1} - E_A)] , \qquad (3)$$

where $a^+_{\mathbf{k}\sigma}$ ($a_{\mathbf{k}\sigma}$) is the creation (annihilation) operator of a nucleon with momentum $\mathbf{k}$ and spin σ; H the intrinsic hamiltonian for interacting nucleons and Ψ^{JM}_A the eigenfunction of the ground state of the Hamiltonian for A nucleon system (with eigenvalue E_A, total angular momentum J and third component M). The function $G^{M\sigma}_f(\mathbf{z})$ in Eq. (3) is the overlap integral

$$G^{M\sigma}_f(\mathbf{z}) = \langle \chi^{1/2}_\sigma, \Psi^f_{A-1}(\mathbf{x}, \ldots, \mathbf{y}) | \Psi^{JM}_A(\mathbf{x}, \ldots, \mathbf{y}, \mathbf{z}) \rangle \qquad (4)$$

between the eigenfunction Ψ^{JM}_A and the eigenfunction Ψ^f_{A-1} (with eigenvalue $E^f_{A-1} = E_{A-1} + E^{f*}_{A-1}$) of the state f of the intrinsic Hamiltonian H, pertaining to the system of $A-1$ interacting nucleons. Since the set of the states f also includes continuum states of the residual

$(A-1)$ nucleon system, the sum over f in Eq. (3) stands for summation over the discrete states of the $(A-1)$ system and integration over the continuum states. The spectral function (3) exactly includes all "final-state interactions" in the states of the $(A-1)$ system, the only plane wave being that describing the relative motion of the knocked-out nucleon and the $(A-1)$ system. The normalization of the spectral function is such that

$$4\pi \int P(k,E) k^2 dk\, dE = 1 . \qquad (5)$$

In order to evaluate the quasielastic section from Eq. (2), the energy conserving δ function can be eliminated by integrating over $\cos\alpha = (\mathbf{q}\cdot\mathbf{k})/(qk)$, obtaining

$$\sigma_2(q,\omega) = 2\pi \sum_{N=1}^{A} \int_{E_{\min}}^{E_{\max}(q,\omega)} dE \int_{k_{\min}(q,\omega,E)}^{k_{\max}(q,\omega,E)} dk\, k\, P_N(k,E)\, \bar{\sigma}_{eN}(q,\omega,k,E) \left| \frac{\partial\omega}{k\,\partial\cos\alpha} \right|^{-1} , \qquad (6)$$

where the limits of integration, fixed by the energy conservation

$$\omega + M_A = \sqrt{M^2 + (\mathbf{k}+\mathbf{q})^2} + \sqrt{M^{*2}_{A-1} + k^2} \qquad (7)$$

with $M^*_{A-1} = M_{A-1} + E^{f*}_{A-1} = E + M_A - M$, are as follows[8]

$$E_{\min} = |E_A| - |E_{A-1}| = M_{A-1} + M - M_A , \qquad (8)$$

$$E_{\max} = M^*_A - M_A , \qquad (9)$$

$$k_{\min} = (\omega + M_A)|k_{CM} - [q/(\omega + M_A)][(M_{A-1} + E^{f*}_{A-1})^2 + k^2_{CM}]^{1/2}|/M^*_A , \qquad (10)$$

$$k_{\max} = (\omega + M_A)\{k_{CM} + [q/(\omega + M_A)][(M_{A-1} + E^{f*}_{A-1})^2 + k^2_{CM}]^{1/2}\}/M^*_A \qquad (11)$$

with $M^*_A = [(\omega + M_A)^2 - q^2]^{1/2}$ being the invariant mass, and

$$k_{c.m.} = \frac{\{[M^{*2}_A - (M_{A-1} + E^{f*}_{A-1})^2 - M^2]^2 - 4(M_{A-1} + E^{f*}_{A-1})^2 M^2\}^{1/2}}{2M^*_A} . \qquad (12)$$

The factor $|\partial\omega/k\,\partial\cos\alpha|$ in Eq. (6), which results from the dependence of $E_2(k_N)$ upon $\cos\alpha$ $[k_N = (k^2 + q^2 + 2kq\cos\alpha)^{1/2}]$, is given by

$$\frac{\partial\omega}{k\,\partial\cos\alpha} = \frac{q}{(M^2 + q^2 + k^2 + 2kq\cos\alpha)^{1/2}}$$

$$= \frac{q}{E_2(k_N)} \qquad (13)$$

and $\bar{\sigma}_{eN}(q,\omega,k,E)$ is the electron-nucleon cross section for a relativistically moving nucleon, averaged over the polar angle, e.g., the one from Ref. 32

$$\bar{\sigma}_{eN}=\frac{\sigma_M}{E_1 E_2}\left\{\left[\frac{q_\mu^2}{q^2}\right]^2\left[\frac{(E_1+E_2)^2}{4}(F_{1N}^2+\bar{\tau}F_{2N}^2)-\frac{q^2}{4}(F_{1N}+F_{2n})^2\right]\right.$$

$$\left.+\left[\tan^2\frac{\theta}{2}+\frac{q_\mu^2}{2q^2}\right]\left[k^2\sin^2\alpha(F_{1N}^2+\bar{\tau}F_{2n}^2)+\frac{\bar{q}_\mu^2}{2}(F_{1N}+F_{2n})^2\right]\right\},\tag{14}$$

where $E_1=\sqrt{M^2+k^2}$, $q_\mu^2=q^2-\omega^2$, $\bar{q}_\mu^2=q^2-(E_1-E_2)^2$, $\bar{\tau}=\bar{q}_\mu^2/(4M^2)$, and σ_M is the Mott cross section. In spite of the fact that in Eq. (6) the factor $E_2(k_N)$ in the denominator of $|\partial\omega/k\partial\cos\alpha|$ cancels exactly with the same factor in the denominator of $\bar{\sigma}_{eN}$, the quantity $(\bar{\sigma}_{eN}|\partial\omega/k\partial\cos\alpha|^{-1})$ still depends upon k and E. Such a dependence, however, is very weak at high momentum transfer [we have checked that the convective term, proportional to $k^2\sin^2\alpha$, which gives a contribution to the cross section less than 5% at $q_\mu^2>0.5$ (GeV/c)^2,[33] becomes negligible at $q_\mu^2>1$ (GeV/c)^2], so that $\bar{\sigma}_{eN}$ and $|\partial\omega/k\partial\cos\alpha|^{-1}$ can be replaced by their values s_{eN} and $|\partial\omega/k\partial\cos\alpha|^{-1}$, respectively, calculated with, e.g., $E_{A-1}^{f*}=0$ (i.e., $E=E_{\min}$) and $k=k_{\min}(q,\omega,E_{\min})$. Therefore Eq. (6) can be written in the factorized form

$$\sigma_2(q,\omega)=(Zs_{ep}+Ns_{en})\left|\overline{\frac{\partial\omega}{k\partial\cos\alpha}}\right|^{-1}F(q,\omega),\tag{15}$$

where the *nuclear structure function* $F(q,\omega)$ is

$$F(q,\omega)=2\pi\int_{E_{\min}}^{E_{\max}(q,\omega)}dE\int_{k_{\min}(q,\omega,E)}^{k_{\max}(q,\omega,E)}P(k,E)\,k\,dk.\tag{16}$$

Using various expressions for the nucleon form factors,[34] we have checked (see, e.g., Ref. 25) that for ^{2}H, ^{3}He, and ^{12}C the factorized cross section (15) differs from Eq. (6) by only few percents in the peak, for $q>3$ fm^{-1}, and by at most 10% in the low-energy side of the peak, for $q>9$ fm^{-1}.

B. The scaling function and the scaling variable

By introducing a new kinematical variable, the *scaling variable* y, which, for the time being, is only required to be a function of q and ω and of no other variables, any dependence upon ω can be expressed as a dependence upon q and y, so that the nuclear structure function (16) can be rewritten as

$$F(q,y)=2\pi\int_{E_{\min}}^{E_{\max}(q,y)}dE\int_{k_{\min}(q,y,E)}^{k_{\max}(q,y,E)}P(k,E)\,k\,dk.\tag{17}$$

The central issue in y scaling concerns the answer to the following questions: (1) under which conditions the quantity $F(q,y)$, which will be hereafter called *theoretical scaling function*, scales in y, i.e., becomes a function of y only?; (2) which is the explicit expression and the physical meaning of the scaling variable?; (3) what kind of information could be provided by the measurement of $F(q,y)$ in a wide range of values of q and y? The answer to these

questions will be given in what follows. The expressions of $E_{\max}$ and $k_{\max}$ given by Eqs. (8)–(12) and the observation that $P(k,E)$ is a rapidly decreasing function of k and E, lead readily to the conclusion that, already for moderate values of the momentum transfer, $E_{\max}$ and $k_{\max}$ can be safely replaced by infinity ($E_{\max}\approx k_{\max}\approx\infty$) in Eqs. (16) and (17). Therefore the q dependence of the structure function (17) will be essentially governed by the q dependence of $k_{\min}$; the latter [Eq. (10)] is determined from the energy conservation [cf. Eq. (7)]

$$\omega+M_A=\sqrt{M^2+(q\pm k_{\min})^2}$$
$$+\sqrt{(M_{A-1}+E_{A-1}^{f*})^2+k_{\min}^2}\tag{18}$$

and therefore is a function of three independent variables: $k_{\min}=k_{\min}(q,\omega,E)$. The positive and the negative sign in front of $k_{\min}$ in Eq. (18) correspond to $\omega>\omega_0$ and to $\omega<\omega_0$, respectively, with $\omega_0=(M^2+q^2)^{1/2}+M_{A-1}^*-M_A$.

Let us suppose that in the process under consideration $E_{A-1}^{f*}=0$, i.e., $E=E_{\min}$ (a physical case will be discussed in the following subsection, while the general case will be considered in Sec. II B 2); then $k_{\min}$ will depend only upon q and ω and therefore, by definition, can represent a scaling variable y, i.e.,

$$|y|=k_{\min}(q,\omega,E_{\min}).\tag{19}$$

The scaling variable satisfies the equation

$$\omega+M_A=[M^2+(q+y)^2]^{1/2}+[M_{A-1}^2+y^2]^{1/2}\tag{20}$$

and has the following explicit expression

$$y=(2M_A^{*2})^{-1}(-q\Delta+\{q^2\Delta^2-4[(\omega+M_A)^2M_{A-1}^2$$
$$-\Delta^2/4]M_A^{*2}\}^{1/2})\tag{21}$$

with $\Delta=M_A^{*2}+M_{A-1}^2-M^2$; as a consequence, $y<0$ corresponds to $\omega<\omega_{\text{peak}}$, and $y>0$ to $\omega>\omega_{\text{peak}}$, with $\omega_{\text{peak}}=(M^2+q^2)^{1/2}+M_{A-1}-M_A$.

Let us note, eventually, that by using the scaling variable defined by Eqs. (20) and (21), the kinematical factor $|\partial\omega/k\partial\cos\alpha|$ in Eq. (15) becomes

$$\left|\overline{\frac{\partial\omega}{k\partial\cos\alpha}}\right|=\frac{q}{E_2(|q+y|)}$$
$$=\frac{q}{(M^2+q^2+y^2+2qy)^{1/2}}.\tag{22}$$

1. Scaling in the two-body system

In the two-body system, one always has $E^{f*}_{A-1} = 0$ ($E = E_{min} = 2.225$ MeV), so that the spectral function is entirely determined by the nucleon momentum distribution $n(k)$, i.e., $P(k,E) = n(k)\delta(E - E_{min})$, and, consequently, $k_{min} = |y|$ for any value of q; the structure function (17) becomes, in this case,

$$F(q,y) = 2\pi \int_{|y|}^{k_{max}(q,y)} n(k) k \, dk \ . \tag{23}$$

Scaling in the deuteron is therefore governed only by the q dependence of k_{max}; for large values of q, such that $k_{max} \approx \infty$, the scaling function (23) reduces to the longitudinal momentum distribution

$$f(y) = 2\pi \int_{|y|}^{\infty} n(k) k \, dk \ . \tag{24}$$

2. Scaling in many-body systems and the role played by nucleon binding

For a many-body system $E^{f*}_{A-1} \neq 0$, so that $k_{min} = k_{min}(q,\omega,E)$ cannot be assumed as a scaling variable, for it depends upon the removal energy E. Therefore there is a certain degree of arbitrariness concerning the definition of the scaling variable, since any k_{min} with a fixed value of E^{f*}_{A-1} depends only upon q and ω and therefore can be chosen as a scaling variable. It is however very useful to adopt, even for a many-body system, the definition given by Eqs. (20) and (21): as a matter of fact, the scaling variable defined in such a way has a very clear physical meaning, since it represents the minimum momentum of nucleons with minimal removal energy. Furthermore, deviations from scaling in this variable, at finite q, can entirely be ascribed (within the PWIA) to the effect of binding, i.e., to the contribution to the qe cross section of nucleons with $E \neq E_{min}$ or, equivalently, to the contribution of the excited states of the final nucleus with energy $E^{*f}_{A-1} > 0$. Indeed, for a complex nucleus the structure function (17) can be rewritten, at finite but large enough values of q, in the following form:

$$F(q,y) = 2\pi \int_{E_{min}}^{\infty} dE \int_{k_{min}(q,y,E)}^{\infty} P(k,E) k \, dk \ . \tag{25}$$

In the asymptotic limit, $q \rightarrow \infty$, one has[8]

$$\lim_{q \rightarrow \infty} k_{min}(q,y,E) = k^{\infty}_{min}(y,E)$$

$$= \left| y + \frac{M^2_{A-1} - M^{*2}_{A-1}}{2[y + (M^2_{A-1} + y^2)^{1/2}]} \right|$$

$$\approx |y - (E - E_{min})| \tag{26}$$

the latter equality holding when $|y| \ll M_{A-1}$ and $E^{f*}_{A-1} \ll M_{A-1}$. Therefore, the asymptotic scaling function for a complex nucleus becomes

$$F(y) = 2\pi \int_{E_{min}}^{\infty} dE \int_{k^{\infty}_{min}(y,E)}^{\infty} P(k,E) k \, dk \tag{27}$$

and scaling in the variable y is recovered. An important difference with respect to the two-body case does however occur: in the latter case the asymptotic scaling func-

tion coincides with the longitudinal momentum distribution [cf. Eq. (24)]. This is not the case for a complex nucleus, for which the longitudinal momentum distribution is given by

$$f(y) = 2\pi \int_{E_{min}}^{\infty} dE \int_{|y|}^{\infty} P(k,E) k \, dk$$

$$= 2\pi \int_{|y|}^{\infty} n(k) k \, dk \tag{28}$$

with

$$n(k) = \int_{E_{min}}^{\infty} P(k,E) \, dE \ . \tag{29}$$

It is clear that the extent to which the longitudinal momentum distribution (28) differs from the asymptotic scaling function (27) depends upon the role played by nucleon binding in quasielastic scattering.

In closing this subsection, we would like to point out that the dependence of k^{∞}_{min} upon E through relation (26) is a consequence of the use of relativistic kinematics to describe the scattering process. When nonrelativistic kinematics is used, the energy conservation equation is

$$\omega = (\mathbf{k} + \mathbf{q})^2/(2M) + \mathbf{k}^2/(2M_{A-1}) + E \tag{30}$$

and the scaling variable becomes[7]

$$|y| = k^{nr}_{min}(E_{min}) \tag{31}$$

$$= |-\mu q + [2M\mu(\omega - E_{min}) + q^2\mu(\mu - 1)]^{1/2}| \ ,$$

where k^{nr}_{min} is the nonrelativistic value of k_{min} and $\mu = M_{A-1}/(M_{A-1} + M)$. In the asymptotic limit one has $\lim_{q \rightarrow \infty} k^{nr}_{min}(q,y,E) = |y|$ for any value of the removal energy, so that the asymptotic scaling function coincides with the longitudinal momentum distribution. The latter limit, however, is reached for $q \gg M$. Indeed, at high but finite values of q one has

$$k^{nr}_{min}(q,y,E) \approx \left| y - \frac{(E - E_{min})M}{q} \right| \tag{32}$$

up to the first order in $(E - E_{min})/q$ and to the second order in y/q. Therefore for $q \leq M$ the identity of $F(q,y)$ and $f(y)$ does not hold and the full expression of $F(q,y)$ has to be used, even within nonrelativistic kinematics.

Hence, the difference between the longitudinal momentum distribution and the asymptotic scaling function is of pure kinematical origin and stems from the necessity of using relativistic kinematics when taking the limit $q \rightarrow \infty$.

3. Approach to scaling, final-state interaction, and the definition of the experimental scaling function

To sum up, the nuclear structure function (16) naturally scales in the variable y defined by Eqs. (20) and (21). If the following definition of the experimental scaling function is adopted

$$F^{exp}_1(q,y) = \frac{\sigma^{exp}_2(q,\omega)}{(Zs_{ep} + Ns_{en})} \left| \overline{\frac{\partial\omega}{k\partial\cos\alpha}} \right| \ , \tag{33}$$

Eq. (15) shows that $F^{exp}_1(q,y)$ will coincide in PWIA with the nuclear structure function (16) and therefore will

scale in y.

We would like to stress that the scaling variable defined by Eqs. (20) and (21) and the scaling function defined by Eq. (33), which naturally follow from the PWIA description of quasielastic scattering, allow one to establish the following model-independent criterion, already formulated in Refs. 25 and 16, concerning the approach to scaling. Since, for fixed values of $y < 0$, E_{max} and k_{max} increase with q, whereas k_{min} decreases, then, *independently of the form of the spectral function $P(k,E)$, the structure function (17) increases with q, until it reaches its asymptotic value given by Eq. (24) for the deuteron, and Eq. (27) for a complex system. Therefore, if the PWIA holds, the experimental scaling function should approach its asymptotic value by increasing with q, i.e., from the bottom; a different approach to scaling would therefore represent a proof of the breaking down of the PWIA at finite q and a clear signature of the presence of FSI.*

A plot of F_1^{exp}, which unifies different sets of data corresponding to rather different kinematics, would therefore allow one to do the following.

(1) To single out the region $(y < 0$, $\omega < \omega_{peak})$ where the qe cross section is mainly determined by nucleonic degrees of freedom, and scaling should be observed, from the region $(y > 0, \omega > \omega_{peak})$ where non-nucleonic degrees of freedom play a dominant role, and y scaling should be grossly violated.

(2) To investigate in great detail, for $y < 0$ and low values of q, the effects from FSI.

(3) To obtain information on the nucleon spectral function and the nucleon momentum distribution from the analysis of the asymptotic scaling function obtained from the inclusive cross section at high values of the momentum transfer.

As far as point (1) is concerned, the usefulness of plotting data in terms of a scaling variable was first illustrated in Ref. 35 using only the few available medium-energy data. It was only in 1980, thanks to the availability of quasielastic cross sections spanning a large range of q and ω, that the concept of nuclear y scaling could be properly tested.[36] Subsequently, the y-scaling analysis was extended[37] to the separate longitudinal and transverse responses. Point (2), i.e., the effects from final-state interactions has been the object of several investigations[13,14]. Finally, point (3) has been studied in Refs. 16 and 17, where the nucleon momentum distribution in ^{2}H and ^{3}He have been obtained; the aim of this paper is to improve the approach adopted in Refs. 16 and 17 and to extend it to the case of complex nuclei (preliminary results can be found in Ref. 38). Before that, let us briefly discuss the scaling variables and functions used by other authors in the framework of relativistic kinematics.

C. Scaling functions and variables used by different authors

Our definitions of the scaling function and of the scaling variable directly result from the PWIA [Eq. (2)] using relativistic kinematics. In principle other definitions could be possible, but in such a case the link with the underlying reaction mechanism is less direct, and the interpretation of the experimental data in terms of nuclear structure properties becomes ambiguous.

The relativistic scaling variable used in this paper [Eq. (20)] coincides with the one first introduced in the analysis of Ref. 36, where it was however interpreted as the component of the nucleon momentum along the momentum transfer (longitudinal momentum component) i.e., $y = (\mathbf{q \cdot k})/q = k_{\parallel} = k \cos\alpha$. Such an interpretation is based on the assumption (see, e.g., Ref. 26) that at high momentum transfer E_{A-1}^{f*} and $k_{\perp}^2$ ($k_{\perp} = k \sin\alpha$ is the momentum component perpendicular to $\mathbf{q}$) can be disregarded in the energy conservation (7). The latter can be written in the following form $(k^2 = k_{\parallel}^2 + k_{\perp}^2)$

$$\omega + M_A = (M^2 + q^2 + k_{\parallel}^2 + k_{\perp}^2 + 2qk_{\parallel})^{1/2}$$
$$+ [(M_{A-1} + E_{A-1}^{f*})^2 + k_{\parallel}^2 + k_{\perp}^2]^{1/2} \quad (34)$$

which shows that $k_{\parallel} = k_{\parallel}(q,\omega,E_{A-1}^{f*},k_{\perp})$, so that in order to have $k_{\parallel}(q,\omega,E_{A-1}^{f*},k_{\perp}) = k_{\parallel}(q,\omega) = y$ one has to assume that E_{A-1}^{f*} and $k_{\perp}^2$ can be disregarded. It can on the contrary be shown that, even in the asymptotic limit $(q \to \infty)$, $k_{\parallel}$ will still depend upon E_{A-1}^{f*} and $k_{\perp}$. As a matter of fact, for a fixed value of y [defined by Eqs. (20) and (21)] we have from Eq. (34), up to first order in $1/q$,

$$k_{\parallel}(q,\omega,E_{A-1}^{f*},k_{\perp}) = y + \frac{M_{A-1}^2 - M_{A-1}^{*2} - k_{\perp}^2}{2[y + (M_{A-1}^2 + y^2)^{1/2}]}$$
$$- \frac{k_{\perp}^2}{4q}\left[1 + \frac{M_{A-1}^{*2} + k_{\perp}^2}{[y + (M_{A-1}^2 + y^2)^{1/2}]^2}\right]$$

$$(35)$$

and then

$$k_{\parallel}^{\infty} = \lim_{q \to \infty} k_{\parallel}(q,\omega,E_{A-1}^{f*},k_{\perp})$$
$$= y + (M_{A-1}^2 - M_{A-1}^{*2} - k_{\perp}^2)/[2y + 2(M_{A-1}^2 + y^2)^{1/2}] .$$

$$(36)$$

Therefore, even if only the terms of the first order in y/M_{A-1}, $k_{\perp}/M_{A-1}$, and E_{A-1}^{f*}/M_{A-1} are retained, one obtains

$$k_{\parallel}^{\infty} = y(1 + E_{A-1}^{f*}/M_{A-1}) - E_{A-1}^{f*}$$
$$- (E_{A-1}^{f*2} + k_{\perp}^2)/2M_{A-1} \approx y - E_{A-1}^{f*} ,$$

so that $k_{\parallel}$ depends strongly on E_{A-1}^{f*} and cannot be adopted as a scaling variable.

The assumption that at high momentum transfer E_{A-1}^{f*} and $k_{\perp}^2$ can be disregarded in the energy conservation not only implies that $k_{\parallel} = y$, but has also a profound impact on the definition of the scaling function. In fact, following this hypothesis, $k_{\parallel}$ would be the only relevant nucleon quantity appearing in the scattering process, and the following relation could be written

$$\sigma_2(q,\omega)d\omega = (Zs_{ep} + N_{s_{en}})f(y)dy \quad (37)$$

with $f(y)$ representing the probability distribution to find a nucleon with momentum $k_{\parallel} = y$. From the above equation the definition of the scaling function used, e.g., in Refs. 26 and 36 would naturally follow

$$F_2^{exp}(q,y) = \frac{\sigma_2^{exp}}{(Zs_{ep} + Ns_{en})} \frac{d\omega}{dy} \tag{38}$$

which differs from the definition (33) in the phase space factor: the one in Eq. (33) is

$$\overline{\partial\omega/k\,\partial\cos\alpha} = q/(M^2 + q^2 + y^2 + 2yq)^{1/2} \tag{39}$$

and results from the use of the correct argument [Eq. (7)] in the energy conserving δ function appearing in Eq. (2), whereas the one in Eq. (38) is

$$d\omega/dy = (q+y)/(M^2 + q^2 + y^2 + 2yq)^{1/2}$$
$$+ y/(M_{A-1}^2 + y^2)^{1/2} \tag{40}$$

and results if, besides the PWIA, the additional approximation of disregarding $k_\perp$ and E_{A-1}^{f*} in the argument of the δ function, is also made.

If the experimental data are analyzed in terms of Eq. (38) (see, e.g., Refs. 18, 26, and 36) and Eq. (37) is considered to be the correct description of the scattering process within the framework of PWIA, then it follows that $F_2^{exp} = f(y)$ [Eq. (28)]. Such an equality, however, does not hold: indeed, due to the fact that, for $y < 0$, $d\omega/dy$ is smaller than $\partial\omega/k\,\partial\cos\alpha$ [cf. Eqs. (39) and (40)], it can be seen that one has $F_2^{exp} < F_1^{exp}$ in the region of interest for y scaling, while in PWIA one has $F_1^{exp} \le f(y)$ [see Sec. II B 2, Eqs. (27) and (28)]. The extent to which F_1^{exp} and F_2^{exp} will differ is given by the value of the ratio $R = (d\omega/dy)(\partial\omega/k\,\partial\cos\alpha)^{-1}$. From Eqs. (39) and (40) it can be seen that $R = 1$ and $F_1^{exp} = F_2^{exp}$ for $y = 0$, whatever the value of the momentum transfer, while for $q \to \infty$ one has $R \to R^\infty = 1 + y/(M_{A-1}^2 + y^2)^{1/2}$; thus for a light system, apart from the point $y \approx 0$, F_1^{exp} and F_2^{exp} will always strongly differ. For a heavy nucleus, one has $M_{A-1}^2 \gg y^2$ and $R^\infty \approx 1$, but at finite momentum transfer $R \approx 1 + y/q$, so that even for a complex nucleus F_1^{exp} and F_2^{exp} are different, e.g., for ^{56}Fe they differ at $q^2 \approx 4$ (GeV/c)^2 and $y = -0.5$ GeV/c by about 30%. Therefore, the extraction of information about nucleon dynamics by using the definition (38) is rather ambiguous.

The issue of the form of the phase space factor to be used in the definition of the scaling function, has been discussed in Refs. 25 and 27, and has again been raised recently in Ref. 29. The results of Ref. 29, where the free electron-nucleon cross section for a nucleon at rest has been used and the removal energy has been disregarded, are a particular case of our general approach in which the scattering takes place off moving nucleons. In this regard, we would like to point out that in recent analyses for complex nuclei[28] the same form of the scaling function as ours, with the proper consideration of the motion of the off-shell nucleon through Eq. (14), has been adopted.

It is also interesting to consider our formalism in the limit of very large nuclei. In this case energy conservation (7) becomes

$$\omega + M_A = [M^2 + (\mathbf{k} + \mathbf{q})^2]^{1/2} + M_{A-1}^* . \tag{41}$$

One readily obtains for $k_- \equiv k_{min}$, $k_+ \equiv k_{max}$ and for the scaling variable y [defined as in Sec. II B by the equation $y = \pm k_{min}(E_{min})$] the same expressions used in Ref. 31,

$$k_\pm(E) = |q \pm [(\omega - E)^2 + 2M(\omega - E)]^{1/2}| , \tag{42a}$$

$$y = -q + [(\omega - E_{min})^2 + 2M(\omega - E_{min})]^{1/2} , \tag{42b}$$

and, once again, one has $k_{min}^\infty = k_-^\infty(E) = |y - (E - E_{min})|$.

In conclusion, our formalism is a very general one, from which various particular cases (e.g., static nucleons[29] and large nuclear masses[31]) readily follow.

III. THE NUCLEON SPECTRAL FUNCTION AND ITS RELATIONS WITH THE SCALING FUNCTION AND THE MOMENTUM DISTRIBUTION

A. The spectral function and the nucleon momentum distribution

As already explained in Sec. II A, the spectral function [Eq. (3)] represents the joint probability to find in the nucleus A a nucleon with momentum k and energy E or, equivalently, the probability that, after a nucleon with momentum k is removed from the target A, the system $(A-1)$ is left with intrinsic excitation energy E_{A-1}^{f*}. It can therefore be represented in the following form[17,25]

$$P(k,E) = P_{gr}(k,E) + P_{ex}(k,E) , \tag{43}$$

where $P_{gr}(k,E) = n_{gr}(k)\delta(E - E_{min})$ yields the probability distribution that the final $(A-1)$ system is left in its ground state (corresponding to $E_{A-1}^{f*} = 0$ and $E = E_{min} = |E_A| - |E_{A-1}|$), whereas $P_{ex}(k,E)$ yields the probability distribution that the final $(A-1)$ system is left in the excited state with excitation energy $E_{A-1}^{f*} = E - E_{min}$ [it is clear that $P_{ex}(k,E)$ vanishes for $E'_{min} > E \ge E_{min}$, where E'_{min} is the removal energy corresponding to the first excited state of the final $(A-1)$ system]. The following exact relations between the spectral function and the momentum distribution $n(k)$ will be used in what follows[2]

$$n(k) = (2\pi)^{-3} \int e^{i\mathbf{k}\cdot(\mathbf{z}-\mathbf{z}')}\rho(\mathbf{z},\mathbf{z}')d\mathbf{z}\,d\mathbf{z}'$$
$$= \int_{E_{min}}^\infty P(k,E)dE = n_{gr}(k) + n_{ex}(k) , \tag{44}$$

where $\rho(\mathbf{z},\mathbf{z}')$ is the nondiagonal one-body density matrix and

$$n_{gr}(k) = \int_{E_{min}}^\infty P_{gr}(k,E)dE = (2\pi)^{-3}(2J+1)^{-1}\sum_{M,\sigma}\left|\int e^{i\mathbf{k}\cdot\mathbf{z}}G_0^{M\sigma}(\mathbf{z})d\mathbf{z}\right|^2 , \tag{45}$$

$$n_{ex}(k) = \int_{E_{min}}^\infty P_{ex}(k,E)dE = (2\pi)^{-3}(2J+1)^{-1}\sum_{M,\sigma}\Sigma_{f\neq 0}\left|\int e^{i\mathbf{k}\cdot\mathbf{z}}G_f^{M\sigma}(\mathbf{z})d\mathbf{z}\right|^2 . \tag{46}$$

Equation (43) holds for any value of A, but for a complex nucleus it is also useful to adopt another representation of the spectral function in which the ground state of the $(A-1)$ system and its excited states represented by one hole excitations are explicitly separated from more complex configurations, e.g., one-particle–two-hole states, which can be reached when two-particle–two-hole states in the target nucleus are considered. One has[39]

$$P(k,E)=P_0(k,E)+P_1(k,E) \ , \tag{47}$$

where

$$P_0(k,E)=(2\pi)^{-3}(2J+1)^{-1}\sum_{M,\sigma}\Sigma_\alpha \left| \int e^{i\mathbf{k}\cdot\mathbf{r}}G_\alpha^{M\sigma}(\mathbf{r})d\mathbf{r} \right|^2 \delta(E-|\epsilon_\alpha|)$$

$$= A^{-1}\Sigma_\alpha A_\alpha n_\alpha(k)\delta(E-|\epsilon_\alpha|) \tag{48}$$

and

$$P_1(k,E)=(2\pi)^{-3}(2J+1)^{-1}\sum_{M,\sigma}\Sigma_{f\neq\alpha} \left| \int e^{i\mathbf{k}\cdot\mathbf{r}}G_f^{M\sigma}(\mathbf{r})d\mathbf{r} \right|^2 \delta(E-E_1^f) \ , \tag{49}$$

where $n_\alpha(k)$ is the hole state momentum distribution with single particle (sp) energy ϵ_α and nucleon number A_α ($\Sigma_\alpha A_\alpha = A$), the sum over α runs only over hole states of the target, and $E_1^f \equiv E_{A-1}^{f*}+E_{\min}$. Within the Hartree-Fock (HF) approximation, $P_1(k,E)=0$, and the HF spectral function, viz.

$$P_0^{\text{HF}}(k,E)= A^{-1}\Sigma_\alpha A_\alpha n_\alpha^{\text{HF}}(k)\delta(E-|\epsilon_\alpha|) \ , \tag{50}$$

is recovered. The main difference between $n_\alpha(k)$ appearing in Eq. (48) and $n_\alpha^{\text{HF}}(k)$, concerns their normalization, or hole state occupation probability $S_\alpha=4\pi\int n_\alpha(k)k^2 dk$; in fact, due to the ground state correlations, $S_\alpha < 1$, whereas $S_\alpha^{\text{HF}}=1$; correspondingly, for a particle state i, $S_i > 0$ and $S_i^{\text{HF}}=0$. For an extended system like nuclear matter, the hole part of the spectral function can be cast in the following form

$$P_0^{NM}(k,E)=3/(4\pi k_F^3)Z(k)\Theta(k_F-k)\delta[E+e(k)] \ , \tag{51}$$

where $Z(k)$ is the hole strength, $e(k)$ the hole single particle energy spectrum and k_F the Fermi momentum [in absence of NN correlations $e(k)=k^2/2M$, $Z(k)=1$ and the usual Fermi gas spectral function is recovered].

Within the representation (47), the nucleon momentum distribution becomes

$$n(k)=n_0(k)+n_1(k) \ , \tag{52}$$

where

$$n_0(k)=\int P_0(k,E)dE, \quad n_1(k)=\int P_1(k,E)dE \ . \tag{53}$$

It should be pointed out that in Eqs. (48) and (51) the finite width of the hole states generated by NN correlations[40] has been disregarded; such an approximation, as argued in Ref. 41, has minor effects on the inclusive cross section we are interested in.

B. Scaling function and momentum distribution

For the two-body system the asymptotic scaling function is given by Eq. (24), from which the momentum distribution can be trivially obtained by a simple derivative

$$n(k)=-\frac{1}{2\pi y}\frac{df(y)}{dy}, \quad k=|y| \ . \tag{54}$$

For $A > 2$, the above equation does not hold and nucleon binding can play a substantial effect. In order to take care of binding effects when extracting $n(k)$ from the scaling function, the following procedure has been adopted.[17] Using Eq. (43), the scaling function (25) becomes

$$F(q,y)=2\pi\int_{|y|}^\infty n_{gr}(k)k\,dk$$

$$+2\pi\int_{E_{\min}}^\infty dE \int_{k_{\min}(q,y,E)}^\infty P_{ex}(k,E)\,k\,dk \ , \tag{55}$$

where the first term trivially scales in y, whereas the second one, because of the explicit dependence of $k_{\min}$ upon the momentum transfer, does not. Such a "scaling violation" is entirely due to the nucleon binding, and, as discussed in Sec. II B, is only present at finite values of q; as a matter of fact, in the asymptotic limit one has [cf. Eq. (27)]

$$F(y)=2\pi\int_{|y|}^\infty n_{gr}(k)k\,dk$$

$$+2\pi\int_{E_{\min}}^\infty dE \int_{k_{\min}^\infty(y,E)}^\infty P_{ex}(k,E)\,k\,dk \tag{56}$$

or, using the representation (47)

$$F(y)=2\pi A^{-1}\Sigma_\alpha A_\alpha \int_{k_{\min}^\infty(y,|\epsilon_\alpha|)}^\infty n_\alpha(k)\,k\,dk$$

$$+2\pi\int_{E_{\min}}^\infty dE \int_{k_{\min}^\infty(y,E)}^\infty P_1(k,E)\,k\,dk \ . \tag{57}$$

Equation (56) can be trivially cast in the form

$$F(y)=f(y)-B(y) \ , \tag{58}$$

where $f(y)$ is the longitudinal momentum distribution (28) and

$$B(y)=2\pi\int_{E_{\min}}^\infty dE \int_{|y|}^{k_{\min}^\infty(y,E)} P_{ex}(k,E)\,k\,dk \tag{59}$$

is the contribution arising from $P_{ex}(k,E)$. Taking the derivative of both sides of Eq. (58), one gets

$$n(k)=-\frac{1}{2\pi y}\left[\frac{dF(y)}{dy}+\frac{dB}{dy}\right], \quad k=|y| \ , \tag{60}$$

where

$$\frac{dB}{dy} = -2\pi y \int_{E_{\min}}^{\infty} dE \left[P_{ex}(|y|,E) - \left[1 - \frac{E - E_{\min}}{y} \right] P_{ex}(k_{\min}^{\infty}(y,E),E) \right] . \tag{61}$$

The quantities $B(y)$ [Eq. (59)] and dB/dy [Eq. (61)] have been called in Ref. 17 the *binding corrections* to the scaling function and to the momentum distribution, respectively. It follows from Eq. (60) that the nucleon momentum distribution can be obtained from y scaling only if the binding correction $B(y)$ and the asymptotic scaling function $F(y)$ are known. For ^{3}He it has been shown in Ref. 17, that in a wide range of y, the binding correction to the momentum distribution is much smaller than the derivative of the scaling function, even if the binding correction to the scaling function has been found to be very large.[42] The same general pattern appears to hold for complex nuclei as well, at least for values of the nucleon momentum $k < 500$ MeV/c, as will be shown in Sec. V.

Furthermore, it is important to realize that for $y < 0$ the sign of the binding correction to the momentum distribution is known both at $y \approx 0$ and at large values of $|y|$: (i) for $y \approx 0$ one has $dB/dy < 0$, because the term proportional to $(E - E_{\min})$ is the dominant one in Eq. (61) and is negative [we wish to recall that $P_{ex}(k,E) \neq 0$ only for $E \geq E'_{\min} > E_{\min}$, see Sec. III A]; (ii) at high negative values of y the integrand function in Eq. (61) is positive, i.e.,

$$P_{ex}(|y|,E) > [1 + (E - E_{\min})/|y|]$$

$$\times P_{ex}\{|y|[1 + (E - E_{\min})/|y|],E\} ,$$

because the spectral function has to decrease faster than k^{-3} at high k, due to the normalization condition [Eq. (5)], and then $dB/dy > 0$. As a consequence, if the binding correction is neglected, one gets a lower bound of the momentum distribution at high k.

The question of the knowledge of the experimental asymptotic scaling function $F(y)$, i.e., the basic quantity which is necessary in order to obtain the nucleon momentum distribution, appears to be a delicate one. As a matter of fact, a careful plot of the experimental data versus the momentum transfer for fixed values of y, shows (see, e.g., Refs. 16 and 17 and Sec. IV) that at large values of y, a clear scaling violation is present, whose origin has to be ascribed to the FSI; in fact, the data *decrease* with momentum transfer, instead of increasing, as predicted by the PWIA (see Sec. II B 3). In Ref. 16, the contribution of the FSI in the deuteron, calculated within an exact treatment of the two-body continuum states,[10] was subtracted from the experimental data and a reliable asymptotic scaling function was obtained. In the case of ^{3}He, for which a full calculation of the FSI in terms of realistic interactions is still waited for, the asymptotic scaling function was obtained in Ref. 17 by considering only the experimental data at the highest values of the momentum transfer. Such a procedure, which entirely relies on the expectation that the available data at high momentum transfer are not affected by the FSI, is not a completely satisfactory one. A more reliable approach is

presented in this paper, where the asymptotic scaling function has been obtained by an extrapolation procedure which, in principle, allows one to obtain the asymptotic scaling function even if the experimental data are affected by FSI. Such an approach is illustrated in the next section.

IV. THE EXPERIMENTAL SCALING FUNCTION AND ITS ASYMPTOTIC VALUE FOR FEW-BODY SYSTEMS AND COMPLEX NUCLEI

Using the definition of the scaling variable according to Eqs. (20) and (21), the relativistic off-shell electron-nucleon cross section σ_{eN} from Ref. 32 and the experimental inclusive cross section σ_2 from Ref. 19 (^{3}He), Ref. 22 (^{4}He, ^{12}C, ^{56}Fe) and Ref. 23 (nuclear matter), the experimental scaling function $F_1^{\exp}(q,y)$ [Eq. (33)] was obtained. The results are presented in Fig. 1 where the well-known general features of the scaling function,[36] namely, a qualitative scaling behavior for $y < 0$ and a gross violation of scaling for $y > 0$, can be seen. It is clear, however, that from such a plot it is hard to assess whether, for a fixed value of $y < 0$, scaling really occurs. In Refs. 16 and 17 the scaling functions of ^{2}H and ^{3}He have been plotted versus q^2 for fixed values of y, and a region where scaling is violated was clearly singled out. As a matter of fact, at high negative values of y, $F_1^{\exp}(q,y)$ exhibits two systematic features: (i) a sharp fall off at low values of q; (ii) a slower, but still persisting decrease at higher values of q. The first feature can be ascribed to the effect of FSI, whereas the second one has been interpreted[42] as the result of the opposite effects of the contribution from FSI and from the high removal energy tail of the spectral function; as a matter of fact, due to the former the scaling function decreases as q increases, whereas due to the latter the scaling function increases. Both features, observed in ^{2}He and ^{3}He, appear to be a general feature of nuclei, as it is shown in Fig. 2, where the values of the experimental scaling function, averaged in a range of ± 50 MeV/c around the fixed values of y, are reported versus q^2 for ^{4}He and ^{56}Fe. Therefore, it is legitimate to raise the question as to whether present experimental data at the highest values of the momentum transfer could be assumed to represent the asymptotic limit of the scaling function. In order to be able to obtain the latter from the available experimental data even if they are affected by FSI, the following approach has been developed (see also some preliminary results presented in Ref. 38). Let us assume that for large values of q, $F_1(q,y)$ can be represented by a series expansion in inverse powers of q

$$F_1(q,y) = F(y) + F_{(-1)}(y)/q$$

$$+ [F_{(-2)}(y)/q^2 + F_{(-3)}(y)/q^3 + \cdots] . \tag{62}$$

The first, q-independent term on the right-hand side

(RHS) represents the asymptotic scaling function, whereas the other, q-dependent terms, include the effects from FSI. At high momentum transfer the terms $F_{(-n)}(y)/q^n$, with $n \geq 2$, go rapidly to zero and it is therefore expected that the effects from FSI are entirely described by the linear term in $1/q$, $F_{(-1)}(y)/q$. Therefore, if the experimental scaling function is plotted versus $1/q$

for fixed values of y and a linear behavior of the data is observed for small values of $1/q$, then $F_1^{\exp}(q,y)$ can be extrapolated to lower values of $1/q$ and the extrapolated value at $1/q = 0$ will represent the asymptotic scaling function, which can therefore be obtained even if the experimental data are affected by FSI.

We would like to point out that an expansion of the
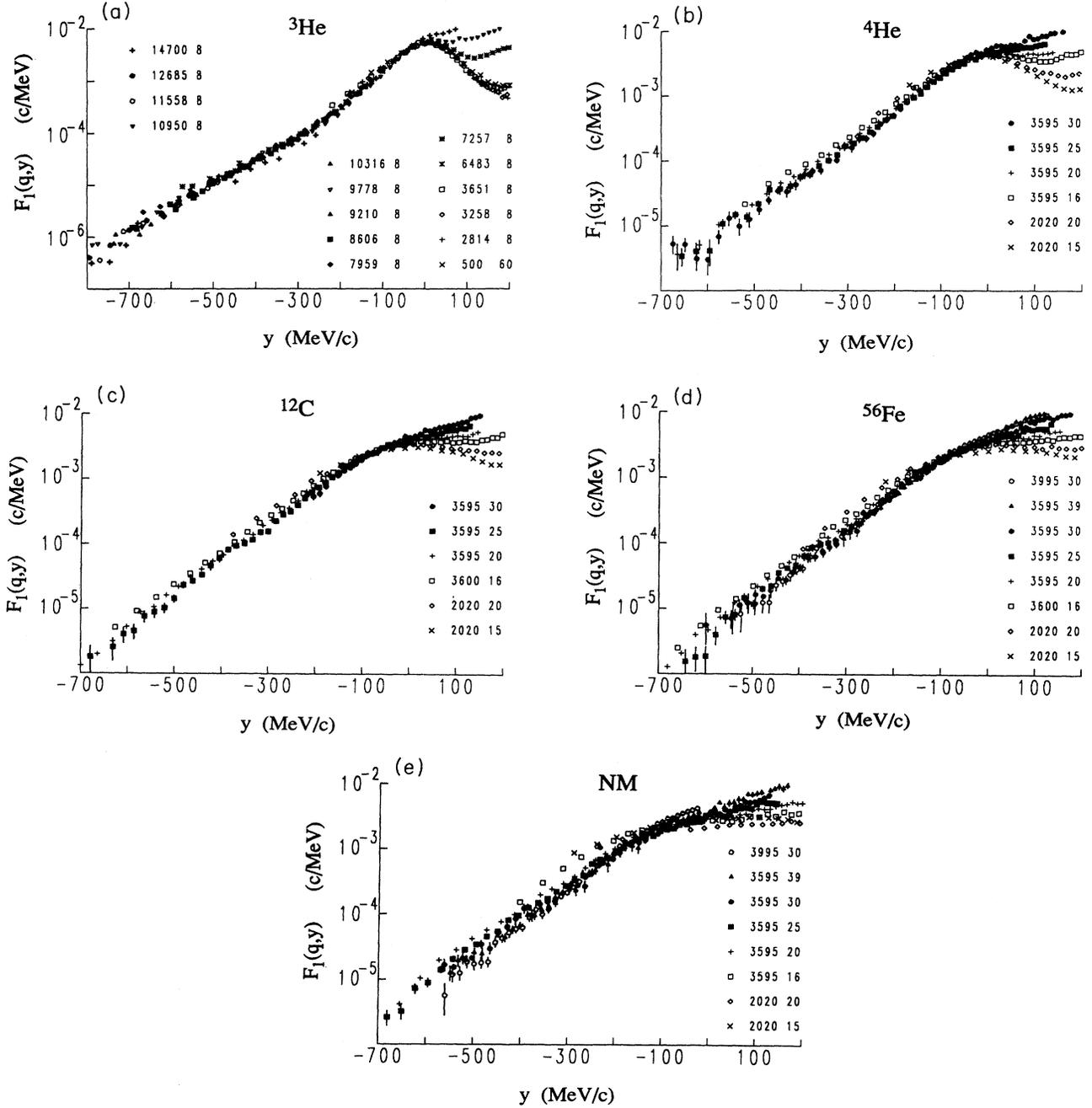
FIG. 1. (a) The scaling function $F_1^{\exp}(q,y)$ [Eq. (33)] of ^{3}He obtained from the experimental data of Ref. 19, using the relativistic off-shell electron-nucleon cross section of Ref. 32 and the nucleon form factors of Ref. 34(a). (b) The same as (a), but for ^{4}He. The data are from Ref. 22. (c) The same as (a), but for ^{12}C. The data are from Ref. 22. (d) The same as (a), but for ^{56}Fe. The data are from Ref. 22. (e) The same as (a), but for nuclear matter. The data are from Ref. 23.

type (62) has been first introduced in Ref. 43 in the study of neutron scattering from liquid Helium, with the aim of obtaining the explicit expressions of $F_{(-n)}(y)$ starting from a theoretical description of the inelastic response. Recently, in Ref. 13 a similar approach has been extended to electron scattering by nuclei adopting nonrelativistic kinematics; in such a case the first term of the expansion is the longitudinal momentum distribution $f(y)$,

whereas $F_{(-1)}(y)$ can be expressed in terms of the elementary NN interaction. In these papers the theoretical convergence of the expansion (62) was investigated by model calculations of the first few terms $F_{(-n)}(y)$; in this paper we attempt at investigating the experimental validity of such a convergence; as a matter of fact, the observation of a linear behavior of $F_1(y,q)$ for large values of q would represent experimental evidence of the conver-
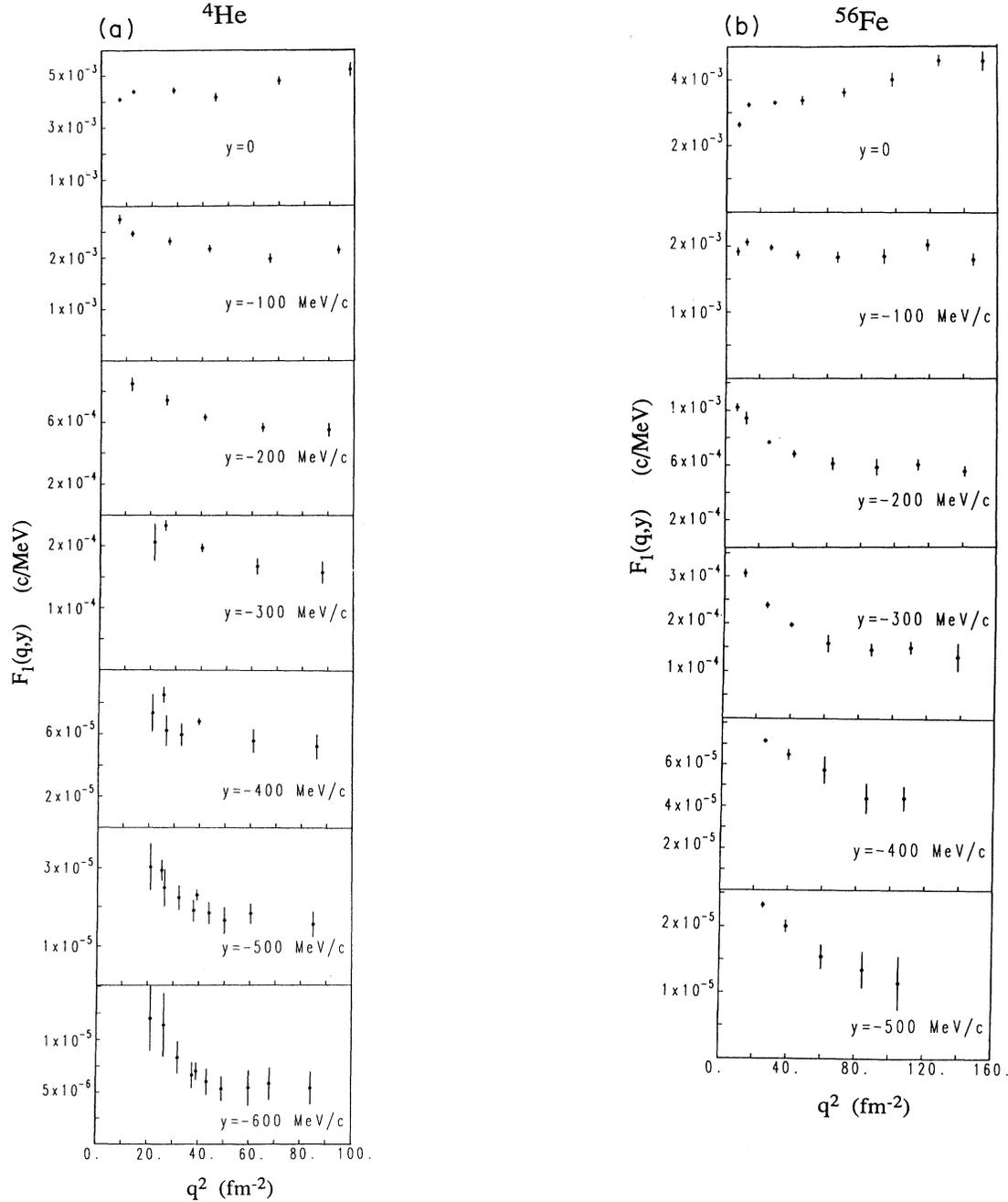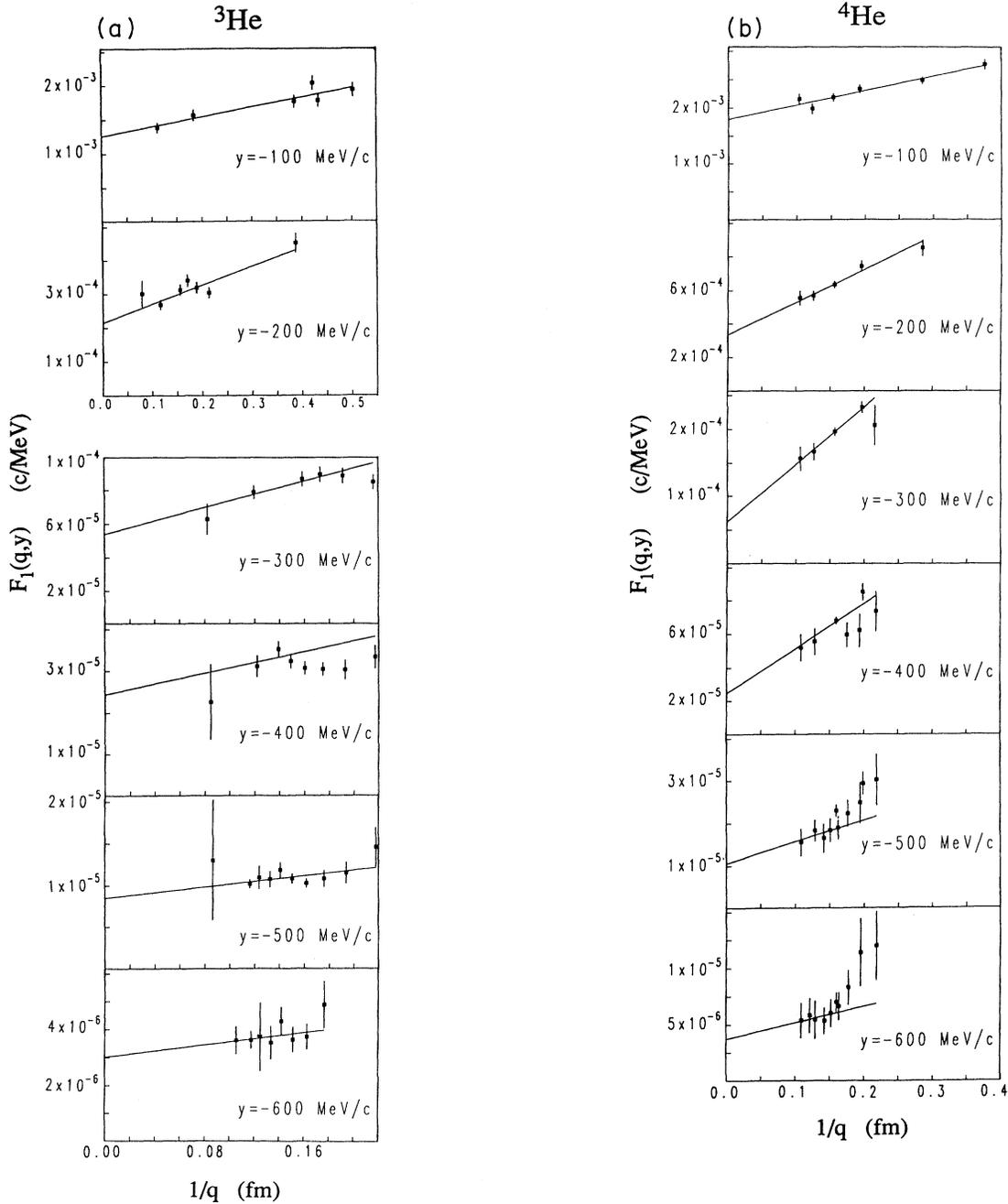

FIG. 2. (a) The experimental scaling function [Eq. (33)] of ^{4}He vs momentum transfer. The data points represent the average values of $F_1^{exp}(q,y)$ in a range of ± 50 MeV around fixed values of y [Eq. (21)]. The relativistic off-shell electron-nucleon cross section and the nucleon form factors are as in Fig. 1(a); the data are from Ref. 19 and Ref. 22. (b) The same as (a), but for ^{56}Fe. The data are the same as in Fig. 1(d).

gence of the expansion (62).

The experimental scaling functions for ^{3}He, ^{4}He, ^{12}C, ^{56}Fe, and nuclear matter, plotted versus $1/q$ for various values of y, are shown in Fig. 3, where the linear fit of the data at low values of $1/q$ is also shown (only data at $y/q < C$, with C ranging from 0.3 to 0.5 for the various nuclei, were considered in the fit). The results presented in these figures deserve the following comments.

(i) For $y \geq -400$ MeV/c, most data show an apparent linear behavior which, for larger values of $|y|$, seems to survive only at 0.1 fm $\leq 1/q < 0.2$ fm.

(ii) Except for ^{3}He and ^{4}He, the quality of the data for $y < -500$ MeV/c is such that a reliable extrapolation to $1/q = 0$ cannot be obtained.

FIG. 3. (a) The experimental scaling function [Eq. (33)] of ^{3}He vs the inverse momentum transfer. The data points represent the average values of $F_1^{exp}(q,y)$ in a range of ± 50 MeV around fixed values of y [Eq. (21)]. The relativistic off-shell electron-nucleon cross section and the nucleon form factors are as in Fig. 1(a). The straight line represents a least square fit of the data at highest momentum transfers (see text). The data are the same as in Fig. 1(a). (b) The same as (a), but for ^{4}He. The data are the same as in Fig. 2(a). (c) The same as (a), but for ^{12}C. The data are the same as in Fig. 1(c). (d) The same as (a), but for ^{56}Fe. The data are the same as in Fig. 1(d). (e) The same as (a), but for nuclear matter. The data are the same as in Fig. 1(e).

(iii) The asymptotic value is systematically lower than the points at the highest values of q; this means that even these points are affected by FSI.

As it is clear from Figs. 1 and 2, at $y = 0$ the scaling behavior strongly deteriorates as q increases, which represents clear evidence of the contribution from inelastic channels, which become dominant at values of the momentum transfer much larger than the value, q_π, corresponding to the pion production kinematical threshold. For example, at $y = 0$ one has $q_\pi = 604$ MeV/c for ^{4}He, whereas a nonscaling behavior begins only at $q \geq 1500$ MeV/c [see Fig. 2(a)]. As one moves to negative values of y, i.e., to $\omega < \omega_{\text{peak}}$, the threshold for inelastic channels increases and such a contamination should decrease (as a matter of fact, for ^{4}He at $y = -500$ MeV/c, one has $q_\pi = 1258$ MeV/c). In order to have a qualitative idea on the contamination from inelastic channels in the data of Fig. 3 at $y < 0$, the following procedure has been adopted:

terms of the type $g_{\text{in}}(y,q) = a(y)(q - q_\pi) + b(y)(q - q_\pi)^2$ or $g_{\text{in}}(y,q) = c(y)(q - q_\pi)^{d(y)}$ were assumed to represent the effect of inelastic channels near the threshold: they were added to Eq. (62) for $q > q_\pi$, and the fitting procedure was repeated, with the result that the obtained values of $F(y)$ change by $\sim 10\%$ for $y < 0$. Such a result seems to be in line with the results of Ref. 18, where the inelastic contributions in the deuteron at $y < 0$ were found to be at most of the order of 20%, for values of the momentum transfer as those considered in this paper. Although a definite answer to the problem of inelastic contributions in complex nuclei can only be given by a dynamical calculation, the situation appears therefore different from the one presented in Ref. 30, where the inelastic channel contributions were viewed as a serious obstacle in extracting information on nucleon properties in the medium from quasielastic inclusive scattering at $\omega < \omega_{\text{peak}}$, since in that work experimental data for ^{2}H
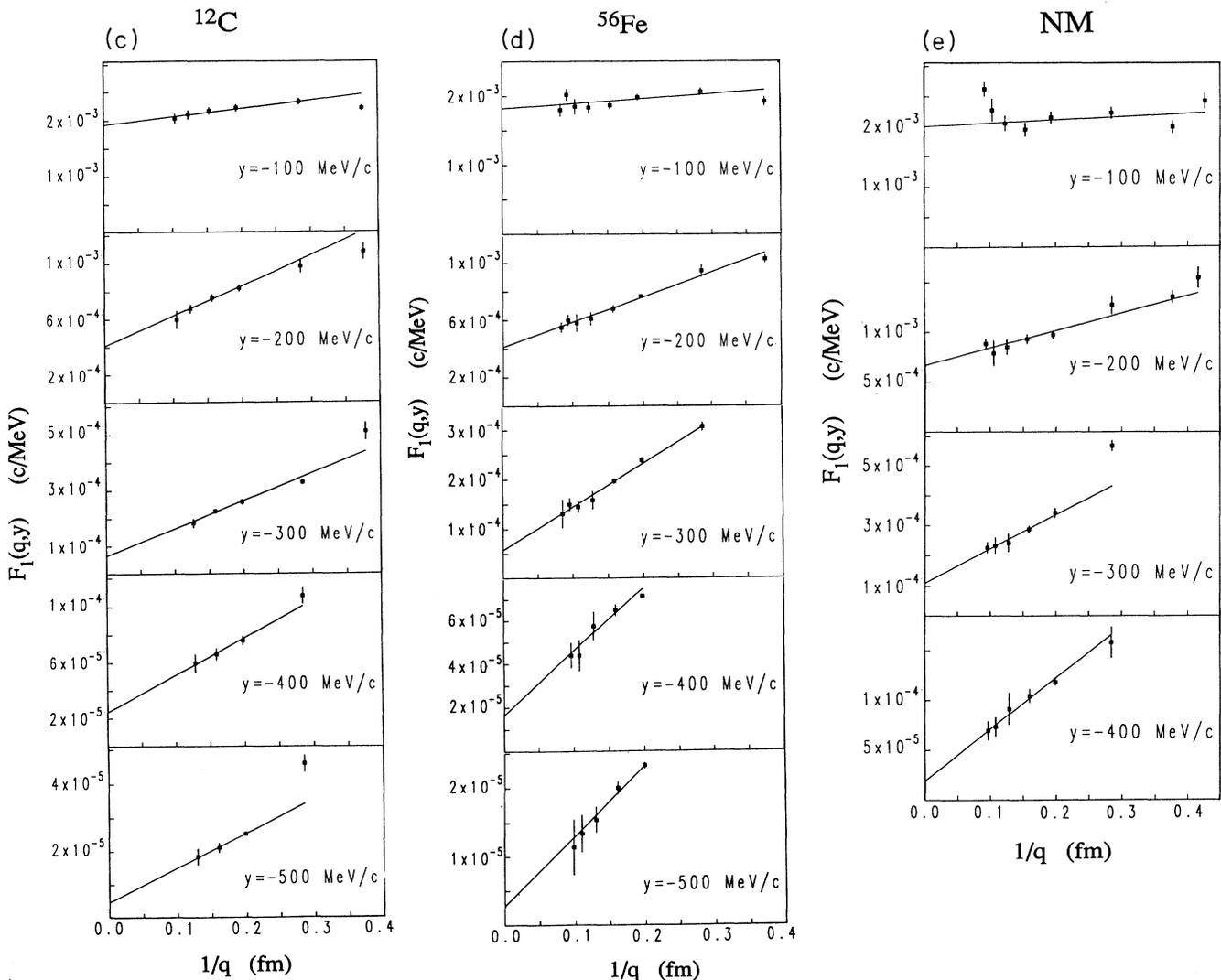

FIG. 3. (*Continued*).

were used up to values of the momentum transfer much higher than those considered here.

The experimental asymptotic scaling functions for ^{3}He, ^{4}He, ^{12}C, ^{56}Fe, and nuclear matter, obtained from the linear fits by the intercepts at $1/q = 0$, are presented in Fig. 4, where the solid lines represent an analytic interpolation that will be used in the next section to obtain the nucleon momentum distribution. It has to be noticed that at large values of $|y|$ the error bars are very large, and that for $y < -500$ MeV/c, the asymptotic scaling function cannot even be determined from the present data, except for ^{3}He and ^{4}He. Experimental data of

higher quality in the region 5 fm$^{-1} \leq q \leq 10$ fm^{-1} would be therefore of extreme usefulness in order to obtain the scaling function for $y \leq -500$ MeV/c and to reduce the uncertainty in its asymptotic value in the region -500 MeV/$c \leq y \leq -300$ MeV/c. We would like to point out, in this respect, that the asymptotic scaling function cannot be simply determined by increasing the value of the momentum transfer, for in the very asymptotic limit $q \to \infty$, also $\omega \to \infty$, and the contribution from the quasielastic cross section to the inclusive cross section will be vanishing, due to the inelastic channels.
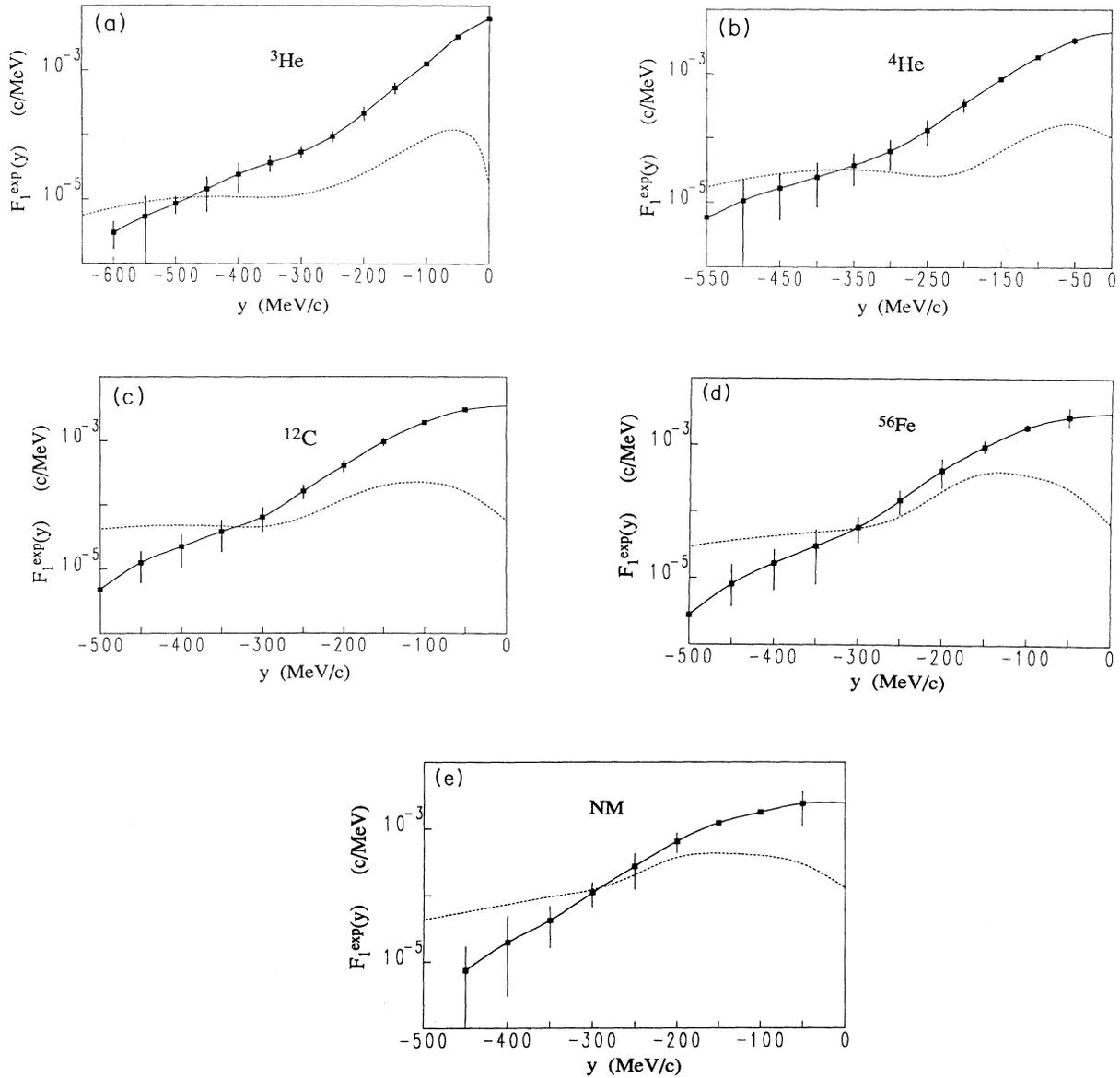

FIG. 4. (a) The experimental asymptotic scaling function of ^{3}He (solid square), obtained using the intercepts of the straight lines shown in Fig. 3(a) [Eq. (62)]; the error bars include the statistical uncertainties on the intercepts. The solid line is a polynomial interpolation of the data. The dashed line is the quantity $B(y)$ [Eq. (59)] calculated with the realistic spectral function of Ref. 2. (b) The same as (a), but for ^{4}He. The dashed line is the quantity $B(y)$ [Eq. (59)] as calculated in Ref. 41. (c) The same as (b), but for ^{12}C. (d) The same as (b), but for ^{56}Fe. (e) The same as (b), but for nuclear matter.

V. THE NUCLEON MOMENTUM DISTRIBUTION

A. Evaluation of the binding correction

Having at disposal the experimental asymptotic scaling function $F(y)$, the momentum distribution can be obtained from Eq. (60), provided the binding correction dB/dy is estimated. The binding correction for ^{3}He evaluated with exact spectral functions turned out to be only a small one, at least up to $k \approx 500$ MeV/c.[17] For the complex nuclei analyzed in this paper, no calculation of the spectral function at the level of accuracy reached in ^{3}He exists so far, apart from nuclear matter, whose spectral function has been obtained by several groups,[40,44,45] in particular in Ref. 40, where relistic NN interactions have been used. In order to have a reliable estimate of the binding correction for complex nuclei, we take advantage of the results of Refs. 46 and 41.

In Ref. 46 a spectral function based on an extended version of the few-nucleon-correlation model of Ref. 47 has been presented and shown to yield results, which, in the region of k and E covered by present experimental data on quasielastic cross sections at $y < 0$, remarkably agree with those predicted by exact spectral functions for ^{3}He and nuclear matter. The general structure of such a spectral function is of the type (47), where $P_0(k,E)$ has the form (48) for finite nuclei and the form (51) for nuclear matter, and $P_1(k,E)$ includes the nucleon momentum and removal energy distributions generated by two-nucleon correlations.

In Ref. 41 this spectral function has been evaluated for ^{4}He, ^{12}C, ^{56}Fe, and nuclear matter using momentum distributions obtained with many-body calculations which employ realistic NN interactions. The results of these calculations lead to hole state occupation probabilities $S_\alpha \approx 0.8$, and particle state probability $S_a \approx 0.2$ for ^{4}He (Refs. 48 and 49) and for ^{12}C (Refs. 6 and 50); these values have also been assumed for ^{56}Fe, while for nuclear matter the values $S_0 = 4\pi \int n_0(k)k^2 dk = 0.75$ and $S_1 = 4\pi \int n_1(k)k^2 dk = 0.25$ (Ref. 40) have been adopted. In Ref. 41 the longitudinal momentum distribution $f(y)$ and the asymptotic scaling function $F(y)$ for ^{4}He, ^{12}C, ^{56}Fe, and nuclear matter have been evaluated using the above spectral functions and obtaining, by this way, the binding correction $B(y) = f(y) - F(y)$. The general results of Ref. 41 agree with the findings of Ref. 42 for ^{3}He: because of binding effects, the longitudinal momentum distributions start to deviate from the asymptotic scaling function at $y \approx -300$ MeV/c, and become an order of magnitude larger at $y \approx -600$ MeV/c. The binding corrections are shown in Fig. 4, whereas in Fig. 5 the longitudinal momentum distributions $f(y)$ and the asymptotic theoretical scaling functions $F(y)$ for ^{4}He and ^{56}Fe calculated in Ref. 41 are compared with the experimental data and with our results for the asymptotic experimental scaling function (similar results have been also obtained for ^{3}He, ^{12}C, and nuclear matter).

The results presented in Figs. 4 and 5, deserve the following comments: (i) the binding correction to the scaling function is very small in the region -150 MeV/$c < y \le 0$, but becomes quite relevant at large values

of $|y|$; this shows that quasielastic cross sections have to be calculated in terms of spectral functions and not simply by convoluting the free electron-nucleon cross section with the nucleon momentum distributions; such an approximation leads to large errors in kinematical regions far from the quasielastic peak (i.e., far from $\omega \approx \omega_{\rm peak}$); (ii) although at $y \le -250$ MeV/c the binding correction to the scaling function is quite an appreciable one, it is fairly constant in a wide range of $|y|$; as a consequence, the binding correction to the momentum distribution, given by the derivative of $B(y)$, is less than 20% for ^{3}He up to $k \approx 500$ MeV/c (Ref. 17) and for ^{4}He and ^{12}C up to $k = 400$ MeV/c, while for ^{56}Fe it is at most 41% and for nuclear matter at most 60% up to $k = 350$ MeV/c; (iii) the theoretical asymptotic scaling function $F(y)$ reasonably agrees with the experimental one, whereas the longitudinal momentum distribution does not; such a disagreement reflects the relevance of the removal energy distribution at large values of $|y|$; (iv) the differences between
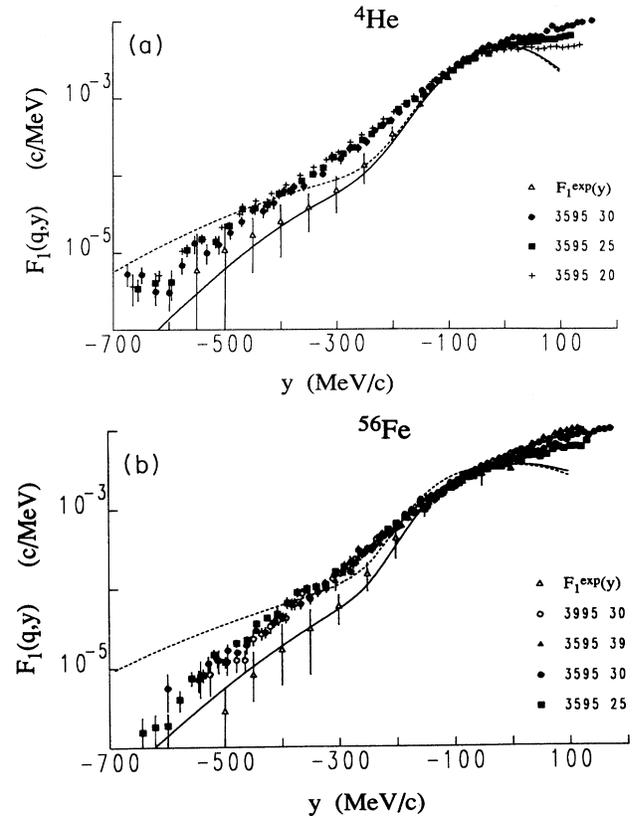

FIG. 5. (a) The experimental scaling function [Eq. (33)] of ^{4}He, obtained from the data at the highest values of the incident electron energy. Triangles represent the experimental asymptotic scaling function $F_1^{\rm exp}(y)$ shown in Fig. 4(b). The solid line is the theoretical scaling function $F(y)$ [Eq. (27)], from Ref. 41; the dashed line is the longitudinal momentum distribution $f(y)$ [Eq. (28)] calculated using the nucleon momentum distribution of Ref. 48. (b) The same as (a), but for ^{56}Fe. Triangles represent the experimental asymptotic scaling function $F_1^{\rm exp}(y)$ shown in Fig. 4(d). The solid line is the theoretical scaling function $F(y)$ [Eq. (27)] and the dashed line is the longitudinal momentum distribution $f(y)$ [Eq. (28)] as calculated in Ref. 41.

the asymptotic experimental scaling function and the data at finite values of q are large, even at $q \approx 2$ GeV/c [except for ^{3}He, see Fig. 3(a)]; this indicates the relevance of the FSI effects even at high, but finite values of the momentum transfer.

In order to reduce the uncertainties due to binding corrections, the measurement of the longitudinal response function, for which the effects from non-nucleonic degrees of freedom are of minor relevance, would be extremely useful, for it would allow to obtain the scaling function both at $y > 0$ and at $y < 0$, where, as it is clear from Eq. (26), binding effects act in opposite directions. The theoretical scaling function for ^{3}He reported in Fig. 6 and calculated with the spectral function of Ref. 2 shows that this is indeed the case and that the binding effect is smaller at $y > 0$.[51] The same result appears to hold for complex nuclei as well.[41] Therefore, complementary information on the momentum distribution can be obtained from the experimental longitudinal scaling function at positive values of y. It would be highly desirable therefore if, in spite of the difficulties related to the Rosenbluth separation, the experiments at high momentum transfer which are under way,[52] could provide some useful information on the scaling function at $y > 0$.

The theoretical results presented so far, were obtained in terms of spectral functions containing the removal energy distribution generated by two-nucleon correlations. For the sake of comparison with Ref. 17, the binding corrections have also been evaluated with model spectral functions in which only the average excitation energy of the final nuclear system is considered, i.e., the spectral function of Eq. (43) with $P_{ex}(k,E) = n_{ex}(k)\delta(E - \bar{E}_{ex})$ for ^{4}He, and the spectral function of Eq. (47) with $P_1(k,E) = n_1(k)\delta(E - \bar{E}_1)$ for complex nuclei; the values of $\bar{E}_{ex}$ and $\bar{E}_1$ can easily be found from the energy weighted sum rule[53,54]

$$E_A / A = |\epsilon_A|$$
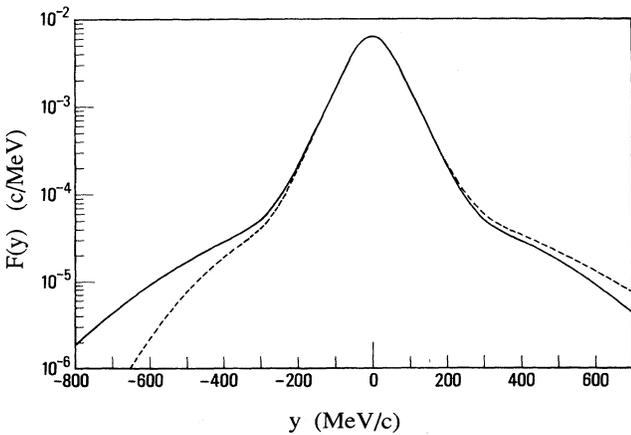$$= (1/2)\{\langle E \rangle - \langle T \rangle (A - 2)/(A - 1) + \langle V_3 \rangle\} , \tag{63}$$

FIG. 6. The theoretical scaling function of ^{3}He (dashed line) for negative and positive values of y, calculated using the spectral function of Ref. 2. The solid line represents the longitudinal momentum distribution $f(y)$ [Eq. (28)].

where

$$\langle T \rangle = \int [k^2/(2M)]P(k,E)\,d^3k\,dE$$

and $\langle E \rangle = \int EP(k,E)\,d^3k\,dE$ are the mean kinetic and removal energies, respectively, $\langle V_3 \rangle$ is the expectation value of the three-body interaction (if any), and $|\epsilon_A|$ is the binding energy per particle. For ^{4}He one has $\langle E \rangle = E_{\min}S_{gr} + \bar{E}_{ex}S_{ex}$ with $S_{gr} = 4\pi \int n_{gr}(k)k^2 dk$ and $S_{ex} = 4\pi \int n_{ex}(k)k^2 dk$, while for complex nuclei, within our assumptions, $\langle E \rangle = E_0 S_0 + \bar{E}_1 S_1$ with $E_0 = A^{-1}\Sigma_\alpha |\epsilon_\alpha| A_\alpha$. Since $|\epsilon_A|$, $\langle T \rangle$, $\langle V_3 \rangle$, $E_{\min}$, ϵ_α, S_{gr}, S_{ex}, S_0, and S_1 are known,[6,48-50] Eq. (63) allows one to readily obtain the values of $\bar{E}_{ex}$ and $\bar{E}_1$. The binding correction to the momentum distribution obtained with these model spectral functions is less than 38% up to $k = 500$ MeV/c for ^{4}He, while it is less than 39% for ^{12}C and less than 58% for ^{56}Fe up to $k = 450$ MeV/c.

B. The nucleon momentum distribution in ^{2}H, ^{3}He, ^{4}He, ^{12}C, ^{56}Fe, and nuclear matter

The nucleon momentum distributions have been obtained by placing in Eq. (60) the asymptotic scaling function obtained in Sec. IV and the binding correction evaluated according to the prescription discussed in the previous section. In Fig. 7 the results for ^{2}H, ^{3}He, ^{4}He, ^{12}C, ^{56}Fe, and nuclear matter are presented separately for each nucleus, whereas in Fig. 8 they are displayed on the same plot (the results for ^{2}H, already published in Ref. 16 and obtained by explicitly taking into account the effects of FSI,[10] are repeated here for the sake of completeness). The solid squares in Fig. 7 represent our results from Eq. (60) including the binding correction. The results obtained by disregarding the binding correction fall within the error bars, which reflect the uncertainties in the determination of the asymptotic value of the scaling function. The momentum distributions obtained by our approach are compared in Fig. 7 with (i) the momentum distributions obtained for ^{2}H, ^{3}He, and ^{4}He, through the exclusive ^{2}H($e,e'p$)n (Ref. 20), ^{3}He($e,e'p$)X (Ref. 21), ^{4}He($e,e'p$)^{3}H (Refs. 55 and 56), and ^{4}He($e,e'p$)X (Ref. 56) reactions; (ii) the momentum distribution $n_0(k)$ [Eq. (53)] obtained from the ^{12}C($e,e'p$)$^{11}B^*$ reactions;[53] (iii) the theoretical momentum distributions obtained within many-body and mean field approaches. In what follows these comparisons will be discussed in detail.

1. ^{2}H and ^{3}He nuclei

The deuteron is an ideal system to check the scaling hypothesis. The reason is twofold: (i) the FSI, i.e., the contribution from the continuum states of the two-body system, can be calculated exactly, and (ii) the y-scaling analysis of the experimental data is free from the ambiguities due to binding effects. The main correction to the inclusive quasielastic (e,e') cross sections at $\omega < \omega_{\text{peak}}$ is represented by the FSI, whose effects have been subtracted in Ref. 16 from the experimental data; on the other hand, the main correction to the PWIA in exclusive $(e,e'p)$ data, arises from FSI and MEC, which, likewise, in Refs. 10 and 20 have been subtracted from the data in
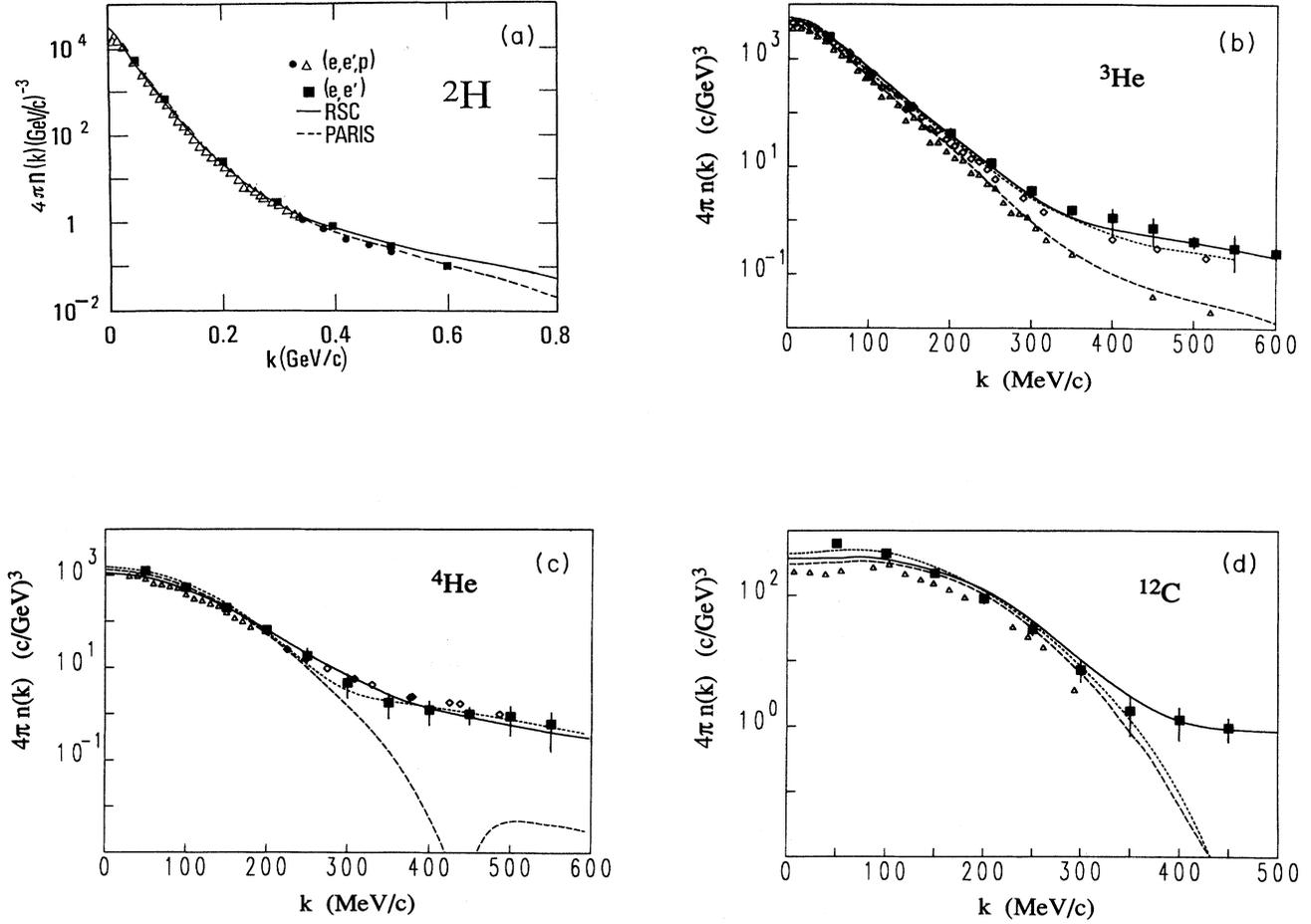
FIG. 7. (a) the nucleon momentum distribution $n(k)$ in the deuteron. Solid squares: $n(k)$ extracted in Ref. 16 from the experimental inclusive cross sections $^2H(e,e')pn$, taking the effects of FSI explicitly into account using the results of calculations from Ref. 10. Triangles and dots: $n(k)$ extracted from the experimental exclusive cross sections in Refs. 10 and 20, respectively. The solid and dashed lines represent $n(k)$ obtained from the RSC (Ref. 57) and Paris (Ref. 58) interactions, respectively. The normalization of $n(k)$ is $\int n(k)d^3k = 1$ (after Ref. 16). (b) The nucleon momentum distribution $n(k)$ in ^3He, obtained from Eq. (60) using the experimental asymptotic scaling function $F_1^{exp}(y)$ shown in Fig. 4(a). Solid squares represent $n(k)$ obtained from Eq. (60), calculating the binding correction [Eq. (61)] with the realistic spectral function of Ref. 2. The error bars include the statistical uncertainties of the asymptotic scaling function [see Fig. 4(a)]. Diamonds and triangles represent $n(k)$ and $n_{gr}(k)$, respectively, as obtained (Ref. 21) from the exclusive processes $^3He(e,e'p)d$ and $^3He(e,e'p)np$ including the FSI and MEC corrections, evaluated according to Ref. 9. Solid and dashed lines: the total proton momentum distribution $n(k)$ [Eq. (44)] and the ground component $n_{gr}(k)$ [Eq. (45)], respectively, as obtained in Ref. 2 from the RSC (Ref. 57) interaction. Dotted line: $n(k)$ as evaluated in Ref. 61, using the Paris (Ref. 58) interaction. The normalization of $n(k)$ is as in (a). (c) The same as in (b), but for ^4He. Solid squares represent $n(k)$ obtained from Eq. (60), calculating the binding correction [Eq. (61)] using the spectral function of Ref. 41. The error bars include the statistical uncertainties of the asymptotic scaling function [see Fig. 4(b)]. Diamonds and triangles represent $n(k)$ and $n_{gr}(k)$, respectively, obtained from the exclusive processes $^4He(e,e'p)^3H$ (Refs. 55 and 56) and $^4He(e,e'p)X$ (Ref. 56). Dotted and dashed lines: $n(k)$ [Eq. (44)] and $n_{gr}(k)$ [Eq. (45)], respectively, obtained in Ref. 48 from the RSC (Ref. 57) interaction. Solid line: $n(k)$ obtained in Ref. 3, using the RSC (Ref. 57) interaction. The normalization of $n(k)$ is as in (a). (d) The same as in (b), but for ^{12}C. The error bars include the statistical uncertainties of the asymptotic scaling function [see Fig. 4(c)]. Triangles represent $n_0(k)$ obtained (Ref. 53) from the exclusive process $^{12}C(e,e'p)^{11}B^*$. Solid and dashed lines: $n(k)$ [Eq. (44)] and $n_0(k)$ [Eq. (53)] obtained in Ref. 6 from the RSC (Ref. 57) interaction. Dotted line: $n(k)$ obtained within the Hartree-Fock approximation [Eqs. (50), (52), and (53)]. The normalization of $n(k)$ is as in (a). (e) the same as in (b), but for ^{56}Fe. The error bars include the statistical uncertainties of the asymptotic scaling function [see Fig. 4(d)]. Solid line: $n(k)$ [Eq. (52)], obtained from the spectral function of Ref. 41. Dotted line: $n(k)$ obtained within the Hartree-Fock approximation [Eqs. (50), (52), and (53)]. The normalization of $n(k)$ is as in (a). (f) The same as (b), but for nuclear matter. The error bars include the statistical uncertainties of the asymptotic scaling function [see Fig. 4(e)]. Solid line: $n(k)$ [Eq. (52)], obtained in Ref. 4(a) from the RSC (Ref. 57) interaction. Dotted line: $n(k)$ for a Fermi gas. The normalization of $n(k)$ is as in (a).
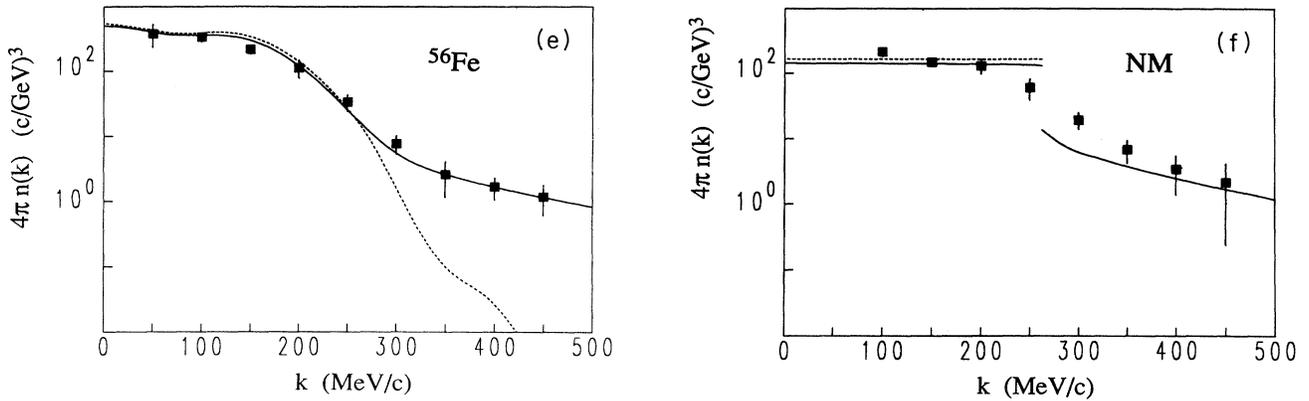
FIG. 7. (Continued).

order to obtain the momentum distribution. It can be seen from Fig. 7(a) that these independent procedures lead to momentum distributions which are in very good agreement with each other; such an agreement, which is a remarkable result in view of the totally different momentum transfer involved in the two experiments ($q < 2.5$ fm^{-1} and $q > 5$ fm^{-1} in exclusive and inclusive experiments, respectively), makes us confident that the quantity shown by the solid squares in Fig. 7(a) does indeed represent the nucleon momentum distribution. The comparison with theoretical momentum distributions, obtained from nonrelativistic wave functions corresponding to Reid soft core[57] (RSC) and Paris[58] interactions, is impressive; it appears therefore that up to $k \approx 600$ MeV/c a nonrelativistic description of the two-body system is in agreement with the experimental data. In order to be able to distinguish between different interactions and to show the possible presence of relativistic effects,[59,60] more accurate experimental data at high values of $|y|$ are needed, which would allow one to investigate the momentum distribution at higher values of k.

As far as ^{3}He is concerned, recent experimental data on the processes ^{3}He$(e,e'p)d$ and ^{3}He$(e,e'p)np$ in the region of removal energy 5.5 MeV $< E <$ 90 MeV allowed one to obtain[21] the separate contributions $n_{gr}(k)$ and $n_{ex}(k)$ and, consequently, the momentum distribution $n(k) = n_{gr}(k) + n_{ex}(k)$. The momentum distribution was also obtained from y scaling in Ref. 17, and found to generally agree with the one resulting from $(e,e'p)$ reactions, except in the region 250 MeV/$c < k <$ 350 MeV/c, where the former turned out to be appreciably higher than the latter. The present, improved analysis of y-scaling data, which, as explained in Sec. IV, allows one to obtain in a model-independent way the asymptotic scaling function, makes clear the origin of such a discrepancy: it was not due to any exotic effect, but it simply arose from our previous analysis of y scaling, in which the asymptotic scaling function was identified with $F(q,y)$ at the highest values of q. According to the results presented in Fig. 3, it is clear that $F(q,y)$ at $q \approx 10$ fm^{-1} is higher than the true asymptotic limit. When the improved asymptotic scaling function shown in Fig. 4(a) is used, the obtained momentum distribution agrees in a satisfactory way with the one resulting from ^{3}He$(e,e'p)X$ reactions, as it can be seen from Fig. 7(b). This figure also shows that (i) as in

the case of the deuteron, the experimental momentum distributions agree very well, up to $k \leq 600$ MeV/c, with theoretical calculations performed with realistic nonrelativistic potential models of the NN interaction;[2,61] (ii) in agreement with the general argument and results of Ref. 2, the high momentum part of $n(k)$ is almost entirely determined by $n_{ex}(k)$, i.e., by that part of the momentum distribution which is generated by NN correlations.

2. ^{4}He and ^{12}C nuclei

The nucleon momentum distributions in ^{4}He and ^{12}C, extracted from our analysis, are compared with the ones obtained from $(e,e'p)$ reactions and with theoretical calculations in Figs. 7(c) and 7(d), respectively. Theoretical momentum distributions for ^{4}He (Refs. 3 and 48) and ^{12}C (Refs. 6 and 50) have been obtained within many-body approaches employing realistic NN interactions. Recent exclusive experimental data on the processes ^{4}He$(e,e'p)^3$H (Refs. 55 and 56) and ^{4}He$(e,e'p)X$ (Ref. 56) in the kinematical region 20 MeV $\leq E <$ 150 MeV, yield preliminary information on $n_{gr}(k)$ and $n_{ex}(k)$ in the region $0 < k < 3$ fm^{-1}; for ^{12}C, exclusive experiments[53] are, on the contrary, still limited to the channel ^{12}C$(e,e'p)^{11}B^*$, which can yield information on $n_0(k)$ only. Some features of the results presented in Figs. 7(c) and 7(d) are in full agreement with the results obtained for ^{3}He, namely, (i) at small values of k, the momentum distribution $n(k)$ is mainly determined by $n_{gr}(k)$ in ^{4}He and by $n_0(k)$ in ^{12}C [dashed lines and triangles in Figs. 7(c) and 7(d)], whereas at high values of k ($k > 350$ MeV/c) it is almost exhausted by $n_{ex}(k)$ and by $n_1(k)$, respectively; (ii) $n_{gr}(k)[n_0(k)]$ obtained from exclusive experiments is lower than the total momentum distribution obtained from inclusive experiments; (iii) for ^{4}He, a qualitative overall agreement between the momentum distributions extracted from inclusive and exclusive data is observed, whereas for ^{12}C, due to the lack of experimental data for the process ^{12}C$(e,e'p)X$ at high values of E, which give information on $n_1(k)$, a full comparison with exclusive data is not possible. For ^{12}C the apparent disagreement between the experimental results and the theoretical calculations at the lowest values of k deserves some comments. As already pointed out in Sec. IV, some contamination by contributions from inelastic channels

might be present in the asymptotic scaling function for low values of $|y|$ and, correspondingly, in the momentum distribution at low values of k. At the same time, the triangles in Fig. 7(d) have been obtained from exclusive experiments by integrating the cross section only in a limited range of removal energies, viz. 15 MeV $< E < 50$ MeV,[53] which, in principle, might not be sufficient to include all the strength, due to the fragmentation of the 1S hole in the residual $(A-1)$ nucleus; moreover, the correction for FSI, evaluated in terms of an unusual optical potential model, might not be a sufficiently accurate one for deep hole states.

The novel feature of our results (which is also common to ^{56}Fe and nuclear matter, see later on) concerns, however, the high momentum part of $n(k)$, which is strongly underestimated by theoretical models based upon the concept of independent particle motion. Since for $k \geq 350$ MeV/c the disagreement between mean field predictions [see the dotted line in Fig. 7(d)] and experimental data concerns orders of magnitude, it is unlikely that it could be ascribed to some drawbacks of the analysis of inclusive and exclusive experimental data in terms of momentum distributions. As far as the analysis of inclusive data is concerned, we wish only to note here that at high k the momentum distribution obtained neglecting the binding correction, which, as already pointed out in Sec. III B, is a lower bound of $n(k)$, is itself orders of magnitude larger than the mean field predictions.

3. ^{56}Fe and nuclear matter

For ^{56}Fe and heavier nuclei, no data exist to date on $(e,e'p)$ reactions. The momentum distributions obtained by our analysis represent therefore the only ones extracted from experimental data which are available at present. The comparison with theoretical momentum distributions [see Figs. 7(e) and 7(f)] shows the same trend observed in lighter systems, namely, an overall agreement, particularly at high values of k, with calculations which include NN correlations and, at the same time, a disagreement by orders of magnitude with mean field results.

Some remarks concerning the results for nuclear matter are also in order: the obtained momentum distribution in the region 200 MeV/$c \leq k \leq 300$ MeV/c, i.e., near the Fermi surface, resembles more the one of a heavy nucleus (e.g., ^{56}Fe), rather than the one of an extended system with a sharp boundary at $k = k_F$. Such a behavior could be ascribed to our procedure for obtaining the momentum distribution from the asymptotic scaling function, which is based upon average values of the experimental scaling function in ranges of ± 50 MeV/c around each value of y (see Sec. IV). As a matter of fact, however, the scaling functions obtained from the experimental cross sections for ^{56}Fe and from the extrapolated data for nuclear matter which are shown in Fig. 1 look very similar in the region 200 MeV/$c \leq k \leq 300$ MeV/c. More and better (e,e') experimental data would be of extreme usefulness in clarifying such a relevant point.

VI. MEAN FIELD APPROACHES, *NN* CORRELATIONS, AND NUCLEON MOMENTUM DISTRIBUTIONS

The relevant effect produced by NN correlations on the one-body nondiagonal density matrix $\rho(\mathbf{z},\mathbf{z}')$, i.e., on the momentum distribution [cf. Eq. (44)], has been discussed in several papers. In Ref. 62 it has been shown that a single Slater determinant cannot reproduce simultaneously the density and the momentum distribution of a correlated system. Such a conclusion was confirmed in Ref. 63 using general arguments based on the experimental[64] and theoretical[4,65] observation of a large depletion of the nucleon Fermi sea. In Ref. 2, starting from the general definition of the momentum distribution in terms of $\rho(\mathbf{z},\mathbf{z}')$, and introducing the overlap integral [Eq. (4)], the exact representation given by Eqs. (43)–(46) has been obtained. Such a representation clearly displays the role of NN correlations: as a matter of fact, it can be clearly seen that, if the ground-state wave function of the target, Ψ_A^{JM}, and the wave functions of the final $(A-1)$ system, Ψ_{A-1}^f, are described by Hartree-Fock Slater determinants, the ground state can couple only to the states of the final $(A-1)$ system which are hole states of the target and, consequently, $P_1(k,E)$ [and $n_1(k)$] will be vanishing. On the other hand, if two-particle–two-hole admixtures generated by correlations are considered, $P_1(k,E)$ [and $n_1(k)$] will differ from zero, due to the coupling of Ψ_A^{JM} to one-particle–two-hole states which are present in Ψ_{A-1}^f.
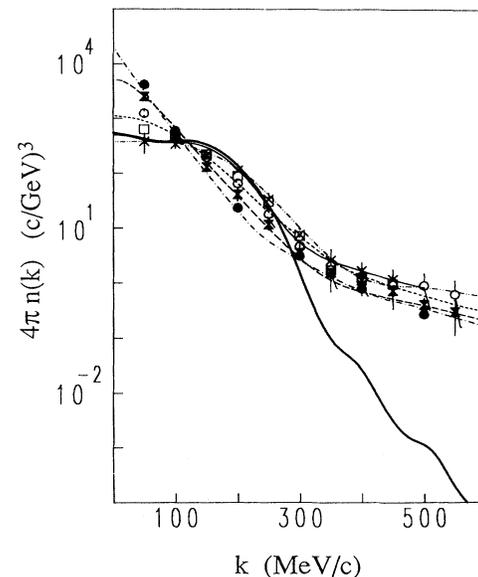

FIG. 8. The nucleon momentum distribution $n(k)$ for ^{2}H ($\bullet$), ^{3}He ($\mathbf{X}$), ^{4}He ($\circ$), ^{12}C ($\square$), and ^{56}Fe ($\times$) obtained from the asymptotic scaling function (see Fig. 7). Dot-dashed line: theoretical $n(k)$ for ^{2}H obtained from the RSC (Ref. 57) interaction; dashed line: $n(k)$ for ^{3}He (Ref. 2); dotted line: $n(k)$ for ^{4}He (Ref. 3); double-dot-dashed line: $n(k)$ for ^{12}C (Ref. 6); thin solid line: $n(k)$ for ^{56}Fe (Ref. 41); and thick solid line: $n(k)$ for ^{56}Fe, evaluated within the Hartree-Fock approximation.

A detailed investigation of the momentum distribution and its relation with the spectral function through Eq. (29), has been presented in Ref. 2 for the case of the three nucleon system described by an exact spectral function. The main outcome of such an investigation was as follows: the momentum distribution at $k \geq 2$ fm^{-1} is entirely exhausted by $n_{ex}(k)$, and, more important, the upper limit of integration, which is necessary to saturate the sum rule [Eq. (27)], sharply increases with k [e.g., for $k > 1.5$ fm^{-1}, the integration over the removal energy must be extended up to an upper limit larger than 50 MeV, while at $k \approx 4$ fm^{-1} an upper limit of 300 MeV is needed (cf. Fig. 3 of Ref. 2)]; this means that the high momentum components are associated with virtual excitations of the "spectator" pair with values of the energy, which are so high that they can be produced only by strong NN correlations. This result appears to be quite a general one, for it has been confirmed in the case of nuclear matter[40] and of complex nuclei.[41]

It is therefore demonstrated that the high momentum components in a nucleus are always associated with high virtual excitations of the spectator ($A - 1$) system, i.e., to the integral of $P_1(k, E)$ for high values of E, much larger than the typical shell-model separation energies; these high excitations are absent in a mean field approach, where the behavior of the momentum distributions is governed by the size of the system and by the values of the single particle energies; this is the reason why, at high values of k, the mean field momentum distributions are orders of magnitude less than the momentum distributions for correlated nucleons. The link between the high momentum components and the high values of the removal energies can be qualitatively explained in terms of the so called two-nucleon correlation model,[47] in which the high momentum components of a nucleon are generated by its hard interaction with a single nucleon, whereas the remaining ($A - 2$) nucleons (the soft nucleons) move in the mean field with center of mass momentum $\mathbf{K}_{A-2} \approx 0$; for a heavy nucleus, for which recoiling energy can be disregarded, the excitation energy of the ($A - 1$) system is therefore centered at $E_{A-1}^{f*} \approx k^2/(2M)$, which, for, e.g., $k \approx 3$ fm^{-1}, is $E_{A-1}^{f*} \approx 200$ MeV $\gg E_0 \approx 20$–30 MeV (see Sec. V A). Such a picture predicts similar behavior of the high momentum part of $n(k)$ independently of A, in agreement with microscopic calculations of the momentum distributions in terms of realistic NN interactions (see Refs. 2–6).

To sum up, the nucleon momentum distributions have very stringent and peculiar features: (i) at low values of k ($k \leq 1$ fm^{-1}), the shape of $n(k)$ for a given value of A is mainly determined by $n_0(k)$ and closely resembles the one predicted by the mean field approach [dashed lines in Figs. 7(d) and 7(e)], apart from the different normalization due to the depletion of the hole states generated by correlations; the shape is different for different nuclei, particularly near $k \approx 0$, due to the different asymptotic behavior of the hole state wave functions; (ii) at high values of k ($k \geq 2$ fm^{-1}), $n(k)$ is, on the contrary, almost entirely determined by $n_1(k)$ and, for the reasons given above in terms of the two-nucleon correlation model, its shape is predicted to be fairly independent of A. It is

very gratifying to see (cf. Fig. 8) that, in spite of the large error bars, the momentum distributions extracted from our analysis clearly display both features. We would like to point out that feature (ii) is not trivial at all, and that its observation by our analysis represents a convincing evidence of correlation effects in nuclei.

VII. SUMMARY AND CONCLUSIONS

In our paper the question has been addressed as to whether the nucleon momentum distribution in nuclei can be obtained from inclusive experiments in the y-scaling region. The answer to such a question is not a trivial one. As a matter of fact, because of FSI effects, which are present at finite values of the momentum transfer, and because of binding effects, which, due to relativistic kinematics, are present even in the asymptotic limit, a direct relation between the momentum distribution and the scaling function at finite q does not exist.

Any attempt at extracting the momentum distribution from y scaling has therefore to face the problem of estimating both the effects from FSI and from nucleon binding. Accordingly, we have developed a method in which: (i) a proper extrapolation procedure of the experimental data is adopted in order to obtain the asymptotic scaling function, even if the available experimental data are affected by FSI effects; (ii) the binding correction to the momentum distribution is explicitly evaluated in terms of spectral functions. By such a procedure the momentum distributions of a series of nuclei, ranging from deuteron to nuclear matter, have been obtained. At large values of the nucleon momentum k, the momentum distributions have large error bars which reflect our poor knowledge of the experimental scaling function in the relevant kinematical ranges. The present experimental data allowed us to determine the nucleon momentum distributions only up to $k \approx 550$ MeV/c for light nuclei, and $k \approx 450$ MeV/c for heavy nuclei; this region, however, is sufficiently wide to make conclusive statements on the breaking down of the mean field theories. As far as the theoretical bias in evaluating the binding correction is concerned, we would like to point out once again that the model dependence due to the evaluation of the binding correction with a specific spectral function does not affect our conclusions, since, as explained in Sec. III B, at high k the momentum distribution extracted from the experimental data with no binding correction represents a lower bound to $n(k)$ and is orders of magnitude higher than the mean field predictions. The agreement with the exclusive ($e, e'p$) data, whenever they exist, and with the results of many-body calculations which include the effects from NN correlations, generated by realistic NN interactions, allows one to draw a consistent picture of the nucleon momentum distributions.

Some remarks are in order concerning kinematics. A consistent treatment would require the use of relativistic kinematics to describe both the scattering process and the bound nucleon dynamics, which appears to be possible, at the moment, only within the relativistic Fermi gas.[66] In our approach full relativistic kinematics together with nonrelativistic spectral functions are used, which might

appear not fully consistent. We believe, however, that our approach is a rational one, since only the region of the spectral function with $k \leq 3$ fm^{-1} is relevant in our analysis.

Given the present accuracy of the experimental data on inclusive cross section, our approach was aimed at investigating only the general, overall features of the nucleon momentum distributions as described in the previous section. More precise data and better estimates of the binding correction would certainly affect our results, but even a 50% modification of the high momentum part of the extracted $n(k)$ would not affect the basic validity of our conclusions. With the advent of new high energy and continuous beam accelerator facilities, it would be possible not only to obtain the nucleon momentum distribution at higher values of momenta, but, at the same time, to carefully investigate possible relativistic effects or differences in the two-nucleon interactions which, at the moment, are both expected to fall within the present large error bars of $n(k)$.

When our paper was almost completed, we became aware of a review paper on y scaling,[67] based on a formalism sharing many points with our approach reviewed in Sec. II B; in particular we would like to point out that the authors of Ref. 67 use a definition of the scaling function, which is the same as the one adopted in this paper [see Eqs. (33) and (39)], so that the experimental scaling functions they obtain fully agree with the ones presented here in Fig. 1.

ACKNOWLEDGMENTS

[1] G. B. West, Phys. Rep. **18**, 263 (1975).

[2] C. Ciofi degli Atti, E. Pace, and G. Salmè, Phys. Lett. **141B**, 14 (1984).

[3] J. G. Zabolitzky and W. Ey, Phys. Lett. **76B**, 527 (1978).

[4] (a) S. Fantoni and V. R. Pandharipande, Nucl. Phys. **A427**, 473 (1984); (b) M. Jaminon, C. Mahaux, and H. Ngo, Nucl. Phys. **A452**, 445 (1986).

[5] J. W. Van Orden, W. Truex, and M. K. Banerjee, Phys. Rev. C **21**, 2628 (1980).

[6] O. Benhar, C. Ciofi degli Atti, S. Liuti, and G. Salmè, Phys. Lett. B **177**, 135 (1986).

[7] C. Ciofi degli Atti, Nuovo Cimento A **76**, 330 (1983).

[8] E. Pace and G. Salmè, Phys. Lett. **110B**, 411 (1982).

[9] J. M. Laget, Phys. Lett. **151B**, 325 (1985) and private communication.

[10] H. Arenhövel, Nucl. Phys. **A384**, 287 (1982); W. Leidemann and H. Arenhövel, private communication.

[11] J. A. Tjon and E. van Meijgaard, Phys. Rev. Lett. **57**, 3011 (1986); Phys. Lett. B **228**, 307 (1989).

[12] M. N. Butler and S. E. Koonin, Phys. Lett. B **205**, 123 (1988); O. Benhar, Proceedings of the 3rd Workshop on Perspectives on Theoretical Nuclear Physics, Cortona, Italy, 1989, edited by L. Bracci et al. (ETS Editrice, Pisa, 1989) p. 140.

[13] S. A. Gurvitz and A. S. Rinat, Phys. Rev. C **35**, 696 (1987); A. S. Rinat and R. Rosenfelder, Phys. Lett. B **193**, 411 (1987); S. A. Gurvitz, A. S. Rinat, and R. Rosenfelder, Phys. Rev. C **40**, 1363 (1989).

[14] R. Cenni, C. Ciofi degli Atti, and G. Salmè, Phys. Rev. C **39**, 1425 (1989); C. Ciofi degli Atti, E. Pace, and G. Salmè, Nucl. Phys. **A497**, 361c (1989).

[15] J. J. Weinstein and J. W. Negele, Phys. Rev. Lett. **49**, 1016 (1982).

[16] C. Ciofi degli Atti, E. Pace, and G. Salmè, Phys. Rev. C **36**, 1208 (1987).

[17] C. Ciofi degli Atti, E. Pace, and G. Salmè, Phys. Rev. C **39**, 259 (1989).

[18] P. Bosted, R. G. Arnold, S. Rock, and Z. Szalata, Phys. Rev. Lett. **49**, 1380 (1982); P. Bosted, private communication.

[19] D. Day et al., Phys. Rev. Lett. **43**, 1143 (1979); S. Rock et al.,

Phys. Rev. C **26**, 1592 (1982).

[20] S. Turck-Chieze et al., Phys. Lett. **142B**, 145 (1984).

[21] E. Jans et al., Phys. Rev. Lett. **49**, 974 (1982); E. Jans et al., Nucl. Phys. **A475**, 687 (1987); C. Marchand et al., Phys. Rev. Lett. **60**, 1703 (1988).

[22] D. Day et al., Phys. Rev. Lett. **59**, 427 (1987) and private communication.

[23] D. Day et al., Phys. Rev. C **40**, 1011 (1989).

[24] G. B. West, Proceedings of the International Summer School on Nuclear Dynamics, Dronten, The Netherlands, 1988 (unpublished); D. Hüber, W. Glöckle, and A. Bömelburg, Phys. Rev. C **42**, 2342 (1990); E. Pace and G. Salmè, and G. B. West (unpublished).

[25] C. Ciofi degli Atti, E. Pace, and G. Salmè, Few-Body Syst. Suppl. **1**, 280 (1986), and references quoted therein.

[26] I. Sick, Progr. Part. Nucl. Phys. **13**, 165 (1984); Nucl. Phys. **A434**, 677 (1985); Phys. Lett. **157B**, 13 (1985); Comments Nucl. Part. Phys. **18**, 109 (1988).

[27] R. G. Arnold et al., Phys. Rev. Lett. **61**, 806 (1988).

[28] D. Day, in the 4th Workshop on Perspectives in Nuclear Physics at Intermediate Energies, edited by S. Boffi, C. Ciofi degli Atti, and M. Giannini (World Scientific, Singapore, 1989), p. 165.

[29] M. N. Butler and R. D. McKeown, Phys. Lett. B **208**, 171 (1989).

[30] G. Yen, A. Harindranath, J. P. Vary, and H. J. Pirner, Phys. Lett. B **218**, 408 (1989).

[31] X. Ji and J. Engel, Phys. Rev. C **40**, R497 (1989).

[32] T. de Forest, Jr., Nucl. Phys. **A392**, 232 (1983).

[33] P. J. Mulders, Phys. Rep. **185**, 85 (1990).

[34] (a) M. Gari and W. Krumpelmann, Phys. Lett. B **173**, 10 (1986); (b) S. Blatnik and N. Zovko, Acta Phys. Austriaca **39**, 62 (1974).

[35] Y. Kawazoe, C. Takeda, and M. Matsuzaki, Progr. Theor. Phys. **54**, 1394 (1975); P. D. Zimmermann, C. F. Williamson, and Y. Kawazoe, Phys. Rev. C **19**, 279 (1979).

[36] I. Sick, D. Day, and J. S. McCarthy, Phys. Rev. Lett. **45**, 871 (1980).

[37] J. M. Finn, R. W. Lourie, and B. H. Cottman, Phys. Rev. C

29, 2230 (1984).

[38]C. Ciofi degli Atti, E. Pace, and G. Salmè, Nucl. Phys. **A508**, 349c (1990).

[39]C. Ciofi degli Atti and S. Liuti, Phys. Lett. B **225**, 215 (1989).

[40]O. Benhar, A. Fabrocini, and S. Fantoni, Nucl. Phys. **A505**, 267 (1989).

[41]C. Ciofi degli Atti, S. Liuti, and S. Simula, Phys. Rev. C **41**, R2474 (1990).

[42]C. Ciofi degli Atti, E. Pace, and G. Salmè, Phys. Lett. **127B**, 303 (1983).

[43]H. A. Gertsch, L. J. Rodriguez, and P. N. Smith, Phys. Rev. A **5**, 1547 (1972).

[44]C. Mahaux and R. Sartor, Nucl. Phys. **A503**, 525 (1989).

[45]A. Ramos, A. Polls, and W. H. Dickhoff, Nucl. Phys. **A503**, 1 (1989).

[46]C. Ciofi degli Atti, L. Frankfurt, S. Simula, and M. Strikman, in *The 4th Workshop on Perspectives in Nuclear Physics at Intermediate Energies* (Ref. 28), p. 312.

[47]L. Frankfurt and M. Strikman, Phys. Rep. **76**, 215 (1981); *ibid.* **160**, 236 (1988).

[48]Y. Akaishi, Nucl. Phys. **A416**, 409c (1984) and private communication.

[49]R. Schiavilla, V. R. Pandharipande, and R. B. Wiringa, Nucl. Phys. **A449**, 219 (1986).

[50]C. Ciofi degli Atti, O. Benhar, and G. Salmè, Proceedings of the 4th miniconference on Nuclear Structure in the $1p$ shell, NIKHEF, Amsterdam, The Netherlands, 1985 (unpublished), p. 209.

[51]C. Ciofi degli Atti, E. Pace, and G. Salmè, contributed papers from The 12th International Conference on Few Body Prob-lems in Physics, Vancouver, Canada, 1989, edited by B. K. Jennings (unpublished), p. G19.

[52]Z. E. Meziani *et al.*, SLAC-NPAS Proposal NE9, 1985 (unpublished); J. P. Chen *et al.*, Bull. Am. Phys. Soc. **33**, 1593 (1988).

[53]S. Frullani and J. Mougey, Adv. Nucl. Phys. **14**, 1 (1984).

[54]S. Boffi, Lett. Nuovo Cimento **1**, 931 (1971); D. S. Koltun, Phys. Rev. Lett. **28**, 182 (1972).

[55]J. F. J. van den Brand *et al.*, Phys. Rev. Lett. **60**, 2006 (1988).

[56]A. Magnon *et al.*, Phys. Lett. B **222**, 352 (1989); J. M. Legoff *et al.*, in *The 4th Workshop on Perspectives in Nuclear Physics at Intermediate Energies* (Ref. 28), p. 376; A. Magnon, private communication.

[57]R. V. Reid, Jr., Ann. Phys. (N.Y.) **50**, 411 (1968).

[58]M. Lacombe *et al.*, Phys. Rev. C **21**, 861 (1980).

[59]F. Gross, Phys. Rev. **186**, 1448 (1969); W. Buck and F. Gross, Phys. Lett. **63B**, 286 (1976).

[60]V. A. Karmanov, Nucl. Phys. **A453**, 707 (1986).

[61]H. Meier-Hajduck, Ch. Hajduck, P. U. Sauer, and W. Theis, Nucl. Phys. **A395**, 332 (1983).

[62]O. Bohigas and S. Stringari, Phys. Lett. **95B**, 9 (1980).

[63]M. Jaminon, C. Mahaux, and H. Ngo, Phys. Lett. **158B**, 103 (1985).

[64]M. Cavedon *et al.*, Phys. Rev. Lett. **49**, 978 (1982).

[65]M. F. Flynn *et al.*, Nucl. Phys. **A427**, 253 (1984).

[66]W. M. Alberico, A. Molinari, T. W. Donnelly, E. L. Kronenberg, and J. W. Van Orden, Phys. Rev. C **38**, 1801 (1988).

[67]D. B. Day, J. S. McCarthy, T. W. Donnelly, and I. Sick, Ann. Rev. Nucl. Part. Sci. **40**, 357 (1990).